# 2025 DRAGON 6 SYMPOSIUM

# 14-18 JULY 2025

## [PROJECT ID. 95373]

## [MARINE DYNAMIC ENVIRONMENT MONITORING COMBINING CONVENTIONAL AND NEW-GENERATION RADAR ALTIMETERS OVER THE COASTAL AND POLAR OCEANS]







<DAY3, 16/JULY/2025>

ID. 95373

PROJECT TITLE: MARINE DYNAMIC ENVIRONMENT MONITORING COMBINING CONVENTIONAL AND NEW-GENERATION RADAR ALTIMETERS OVER THE COASTAL AND POLAR OCEANS

PRINCIPAL INVESTIGATORS: PRO. OLE ANDERSEN, DTU, DENMAK (EUROPEAN PI)
DR. JUNGANG YANG, FIO, MNR, CHINA (CHINESE PI)

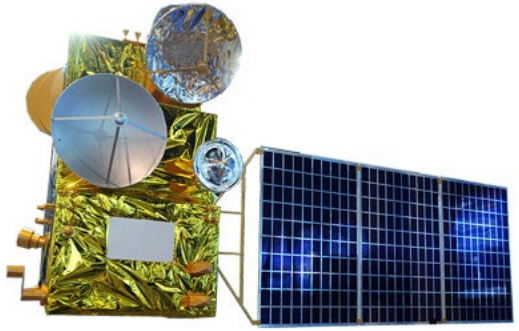
CO-AUTHORS: DR. YONGJUN JIA (NSOAS, CHINA);
DR. SHENGJUN ZHANG (NORTHEASTERN UNIVERSITY, CHINA);

PRESENTED BY: JUNGANG YANG, FIO, MNR, CHINA

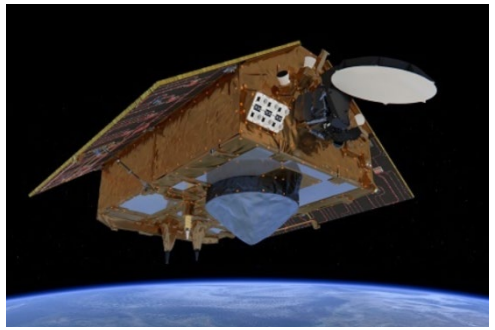
# Objectives

- To explore the data processing and application of satellite radar altimeters by combining the conventional and new-generation altimeters for high-resolution marine dynamic environment monitoring over specific areas.
- To reconstruct 3D ocean temperature and salinity in upper ocean with deep-learning method based on SSH, SST, SSS data.

① Data processing and application of multi-type altimeters in the coastal and polar regions.
② Extraction of the characteristics of submesoscale eddies/currents.
③ Fine-scale marine gravity recovery over coastal zones.
④ Reconstruction of subsurface 3D temperature and salinity.



HY-2B/C/D



Sentinel-6



Sentinel-3A/B



SWOT (Surface Water and Ocean Topography)

# Dragon 6 EO Data Delivery

Altimeter data of Sentinel-3A/3B and Sentinel-6 from Europe and altimeter data of HY-2 series satellites from China are used in this study.

| ESA /Copernicus Missions | No. Scenes |
|---|---|
| 1. SENTINEL-3A/B SRAL Altimetry | L2 products during the period of Dragon 6 |
| 2. SENTINEL-6 | L2 products during the period of Dragon 6 |
| 3. | |
| Total: | |
| Issues: | |

| ESA Third Party Missions | No. Scenes |
|---|---|
| 1. CRYOSAT-2 | L2 products during the period of Dragon 6 |
| 2. SMOS | all archived L2 data |
| 3. | |
| Total: | |
| Issues: | |

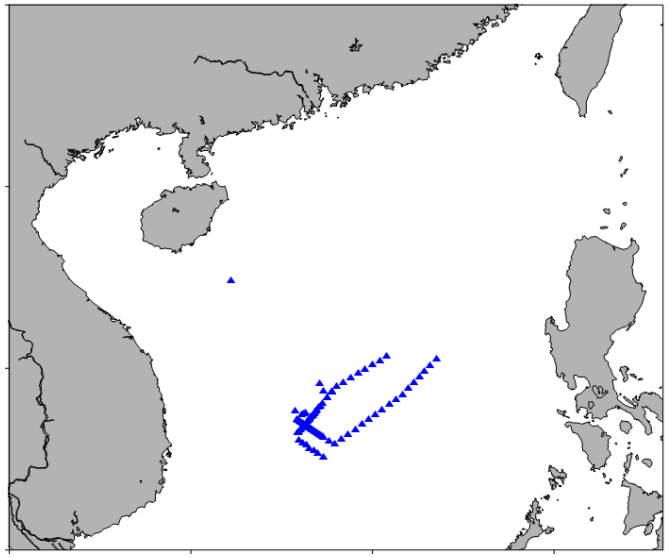
| Chinese EO data | No. Scenes |
|---|---|
| 1. HY-2B ALT | L2 products during the period of Dragon 6 |
| 2. HY-2C ALT | L2 products during the period of Dragon 6 |
| 3. HY-2D ALT | L2 products during the period of Dragon 6 |
| Total: | |
| Issues: | |

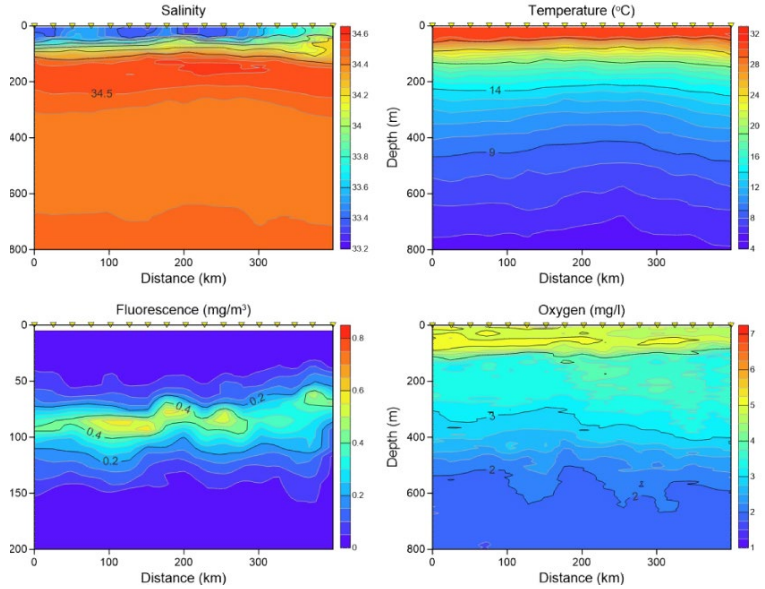
In addition, SWOT altimeter data , SMOS data, SST and SSW data, Reanalysis data, T-S profile data are also used in this study.

# Field Data Collection Campaigns

In June 2024, the scientific research vessel (XIANG YANG HONG 01) of FIO carried out on-site observations of marine environmental parameters (including ocean temperature, salinity, current and so on) in the South China Sea.







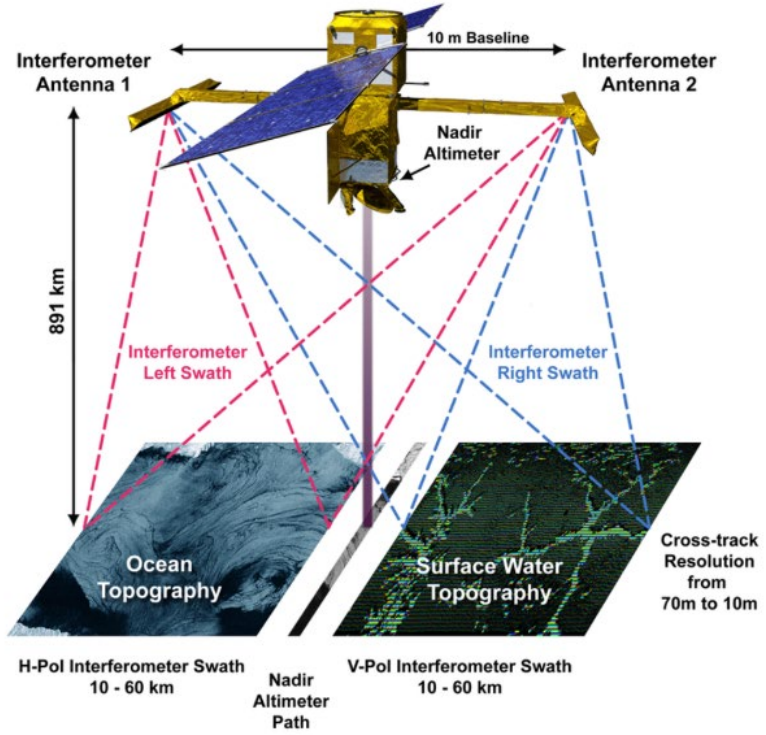
# 1. Evaluation and Analysis of SWOT data

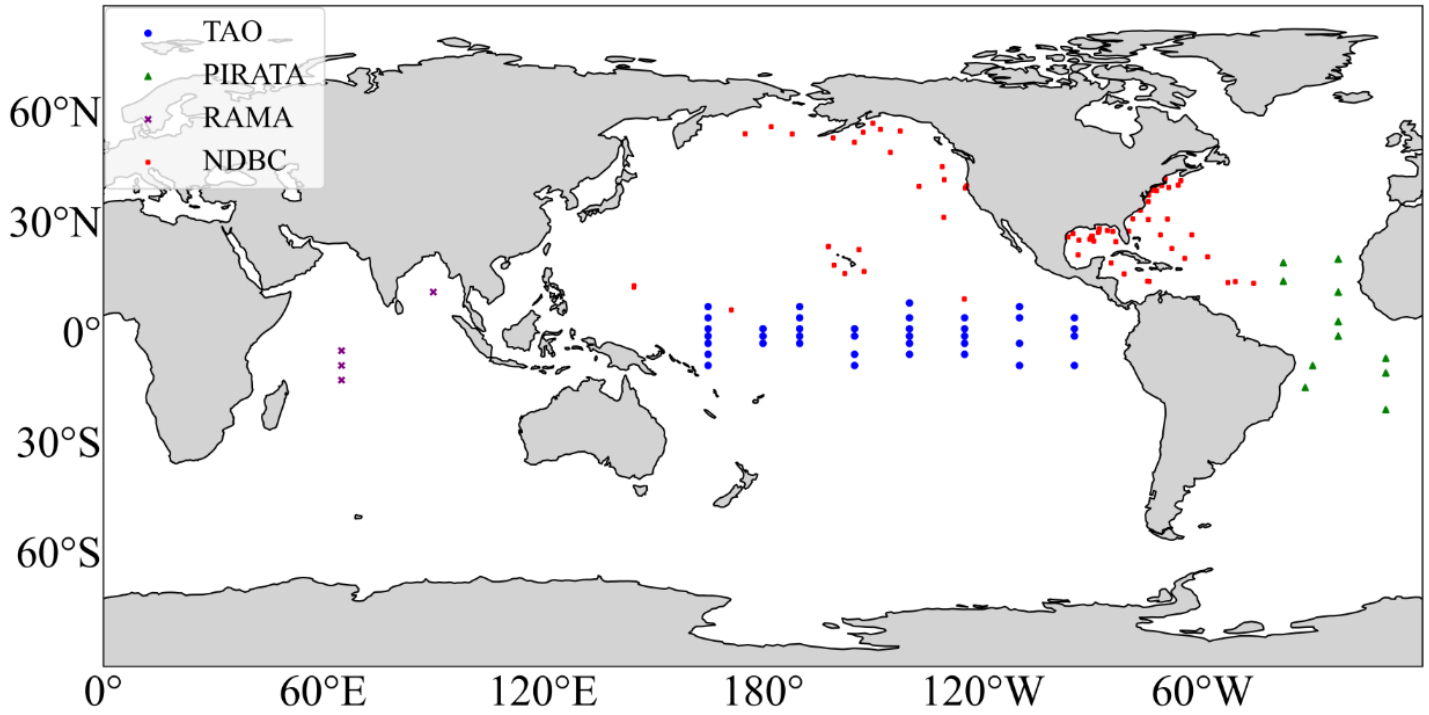
## 1.1 Evaluations of SWOT Significant Wave Height (SWH) and Wind Speed (WS) Data

**SWOT Data**: Level 2 (*l2_lr_ssh WindWave*) products during the period of Nov. 2023-Mar. 2025, 2-km resolution.

**Buoys**: NDBC , TAO, PIRATA and RAMA(Offshore>50 km, water depth>100 m).

**Data collocation**: spatiotemporal matching window of 30 min and 25 km.



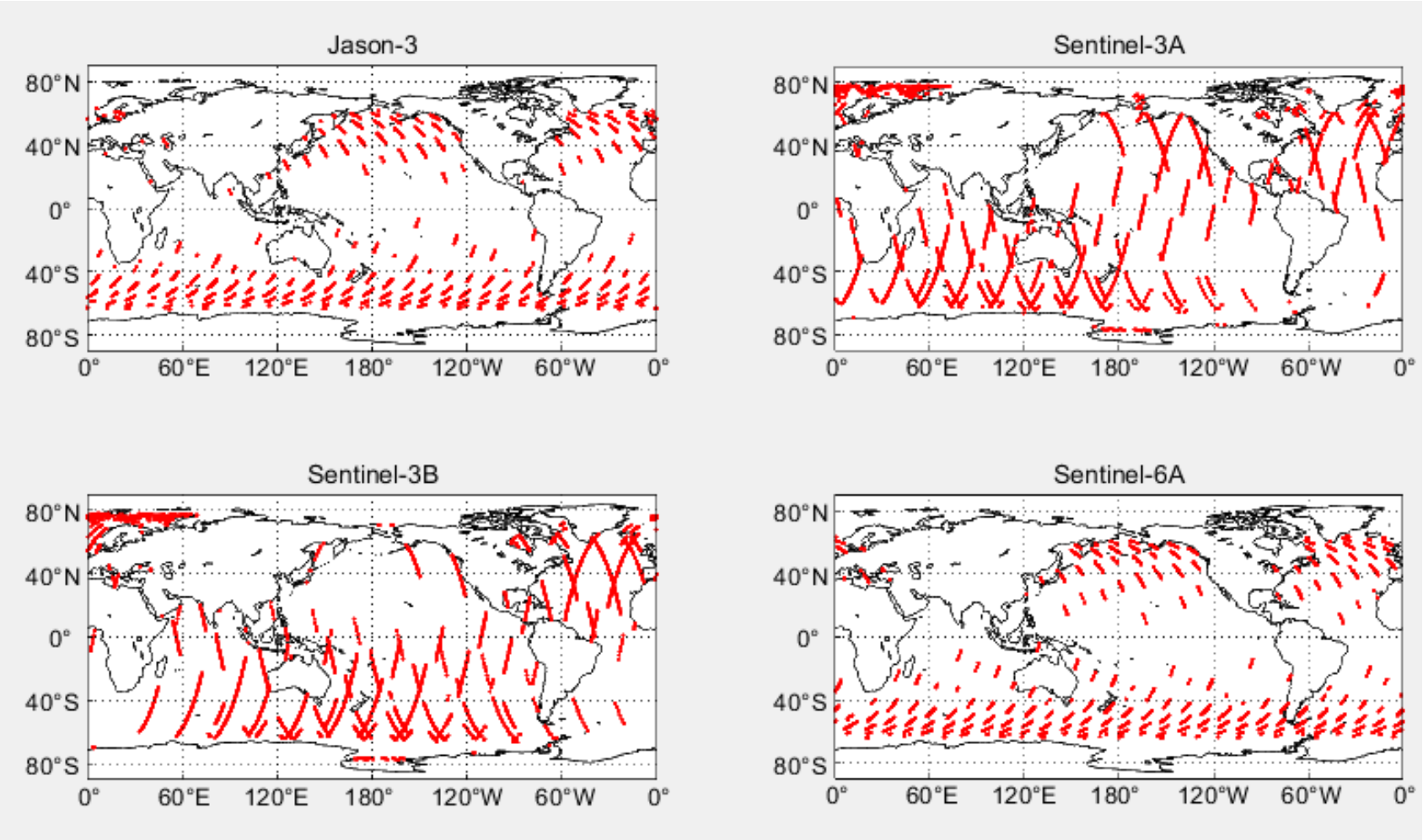




Distribution of the selected buoys

# 1. Evaluation and Analysis of SWOT data

**Nadir Altimeters**: Jason-3, Sentinel-3A/B and Sentinel-6A during the period of Nov. 2023-Nov. 2024.

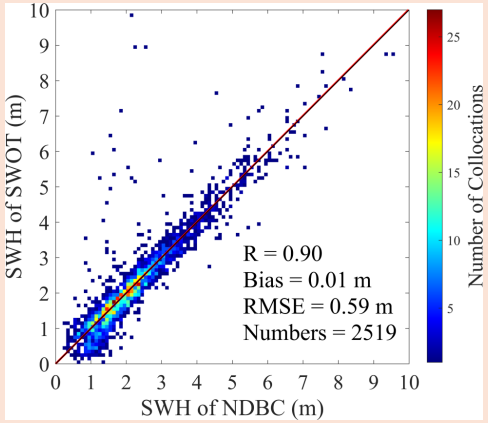
**Data collocation**: spatiotemporal matching window of 30 min and 25 km.

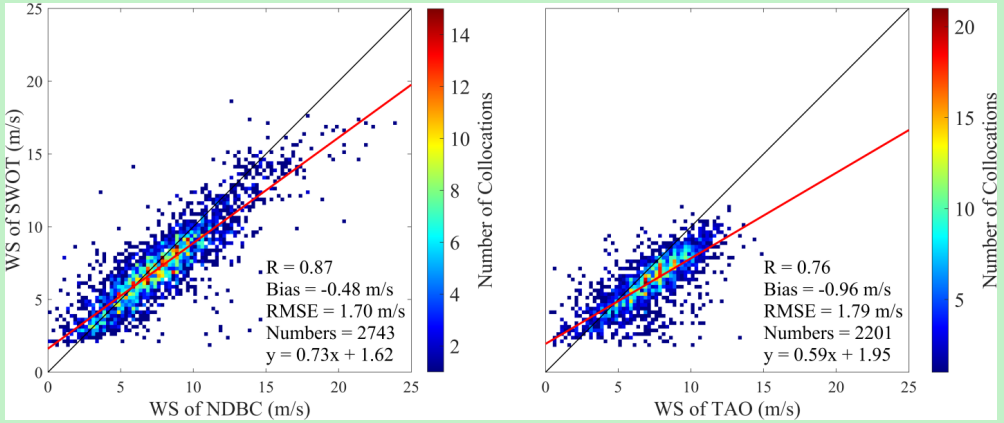



Distribution of the matched data of nadir altimeters

# 1. Evaluation and Analysis of SWOT data

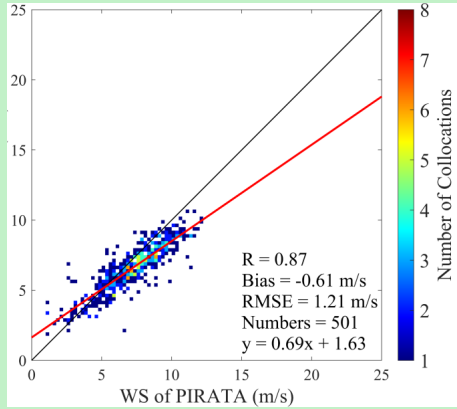
## ➢ Comparisons between SWOT and buoys

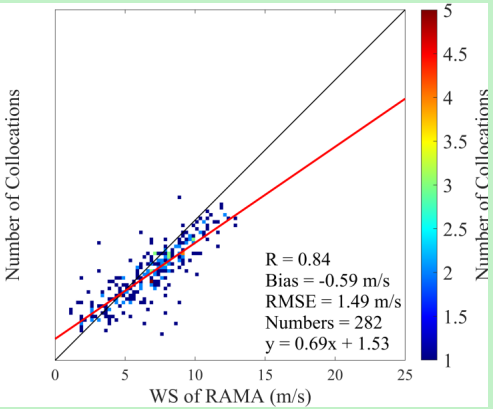


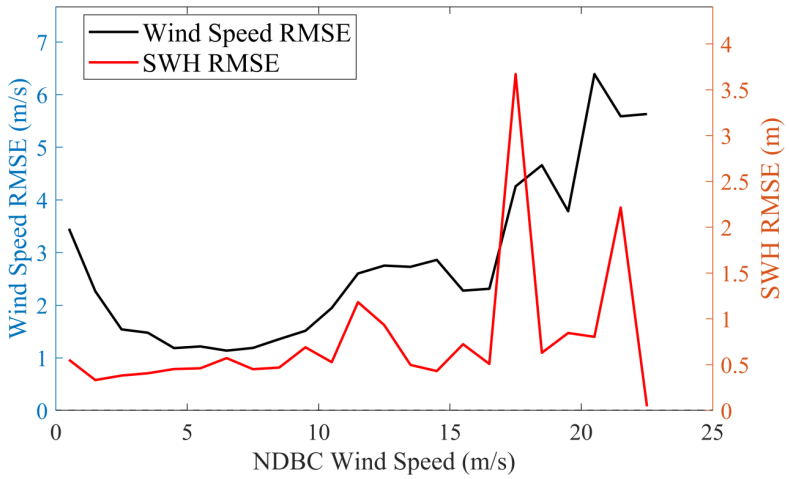









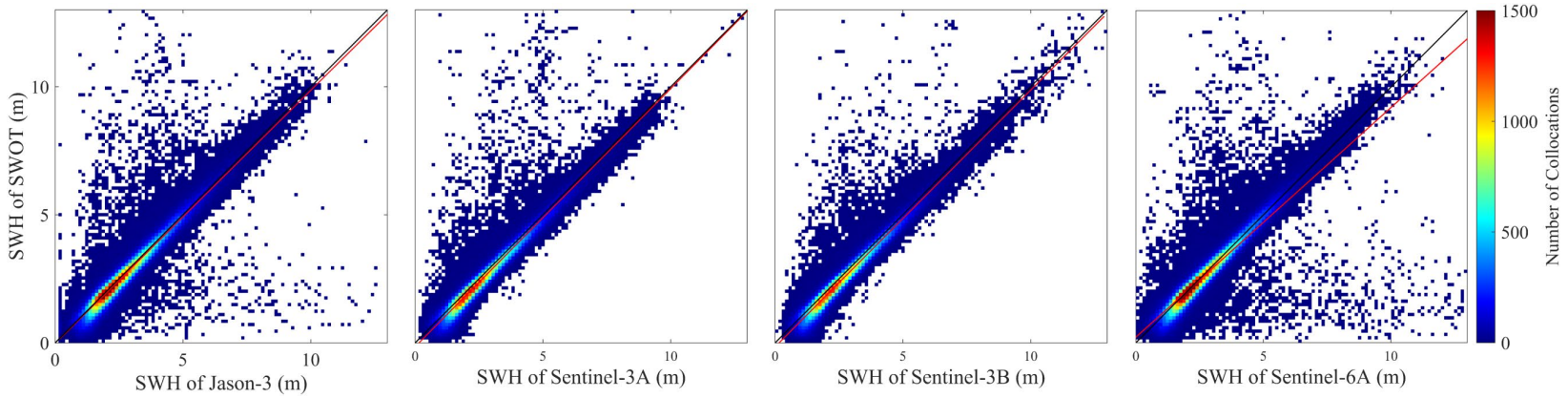




- The RMSE of SWH is 0.59m. The RMSE of WS is 1.21–1.79 m/s.
- The SWOT SWH and WS data have the similar accuracy to the conventional nadir altimeter.
- lower RMSE in the open ocean and higher errors in coastal areas.
- Variabilities of SWH and WS RMSE are consistent under moderate ocean conditions.

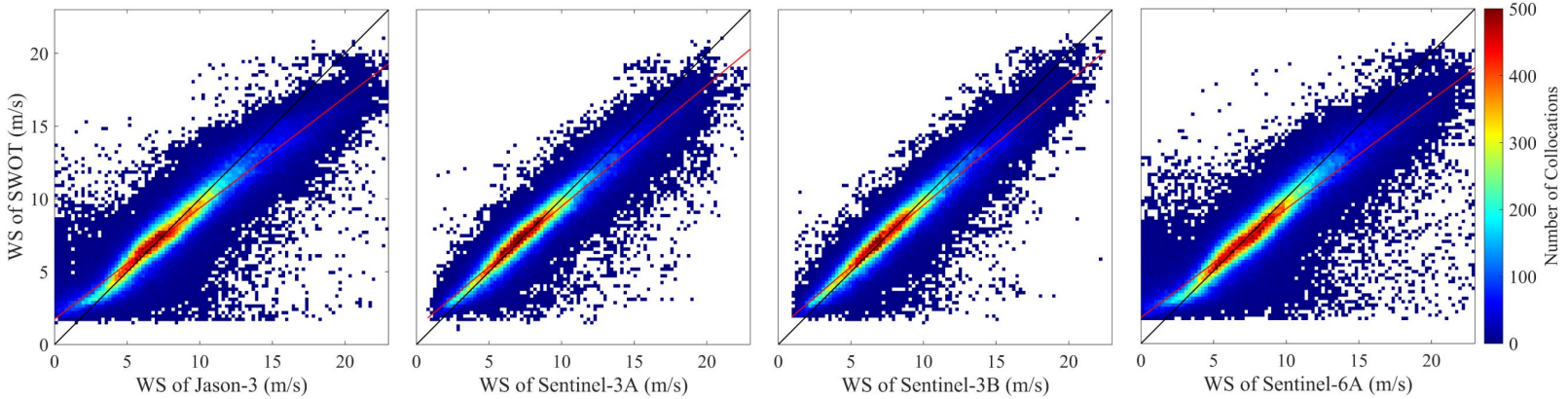
# 1. Evaluation and Analysis of SWOT data

## ➢ Comparisons between SWOT and nadir altimeters




Comparisons of SWH

- Bias: −0.06 ~ −0.15 m.
- RMSE: 0.42~0.69 m.
- larger errors at SWH <2 m.
- Best accuracy for SWH 2–5 m.




Comparisons of WS

- Bias: −0.15 to −0.30 m/s.
- RMSE: 1.17–1.76 m/s.
- SWOT overestimates low WS (<2 m/s), underestimates high WS (>15 m/s).

R. Dong, J. Yang, W. Cui and Q. Chen. Accuracy Assessment of SWOT Wind and Wave Data by Comparison With Buoy and Nadir Altimeter Data. *IEEE Geoscience and Remote Sensing Letters*, 2025, 22:1-5. doi: 10.1109/LGRS.2025.3575212

# 1. Evaluation and Analysis of SWOT data

## 1.2 Analysis of the submeso-scale Resolution Capability of SWOT

**SWOT DATA**: Level 3 (*l3_lr_ssh Basic*) products of Cycles 009 (Jan), 014 (Apr), 018 (Jul), 022 (Oct) 2024.

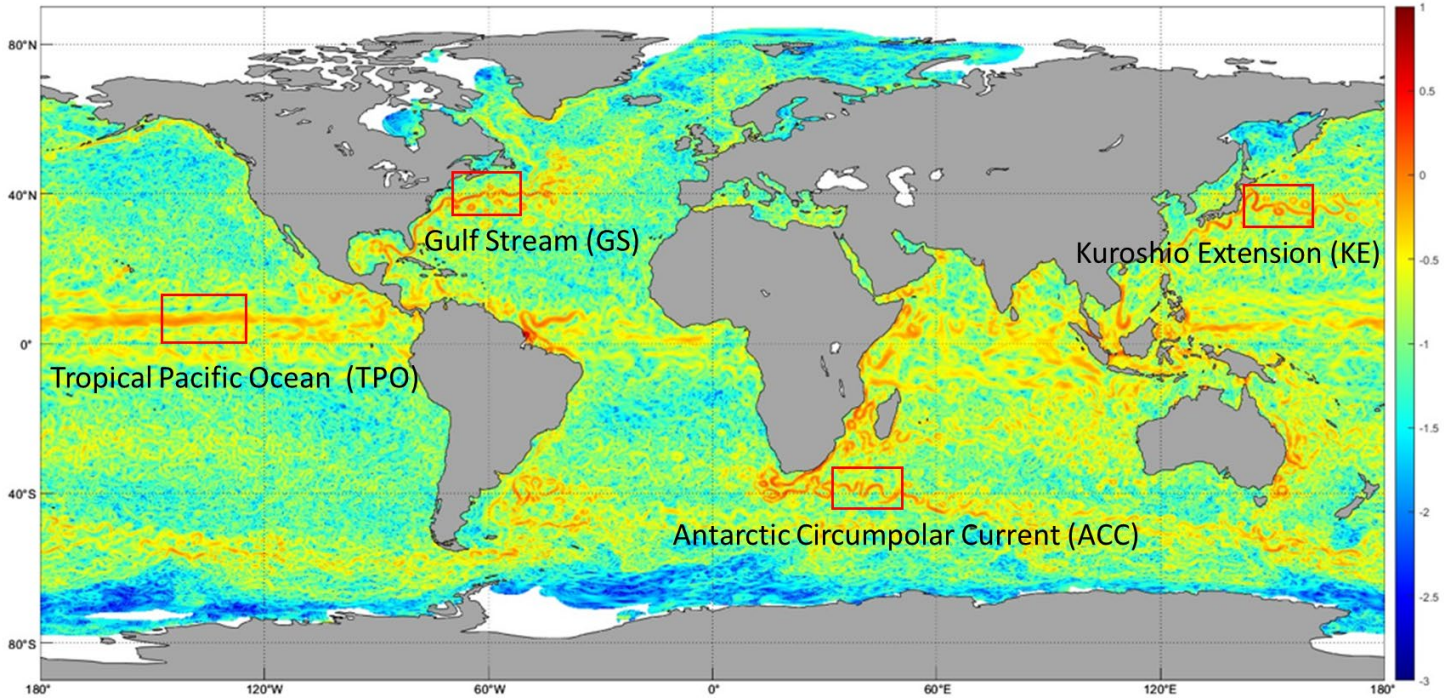
**Sentinel-6 DATA**: Corresponding monthly segments in 2024 for comparison.

### Method

- Wavenumber Spectral Analysis by calculating 1D PSD by Welch's method along the tracks.
- PSDs are averaged to obtain regional-mean spectra.

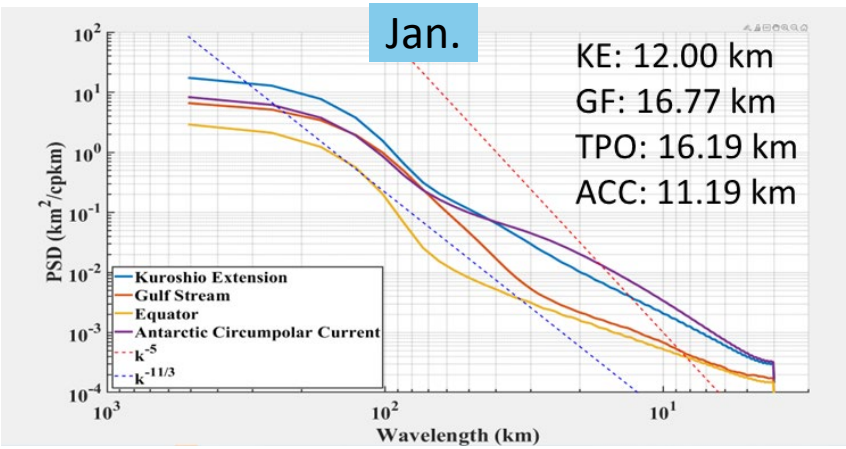
### Resolution Capability

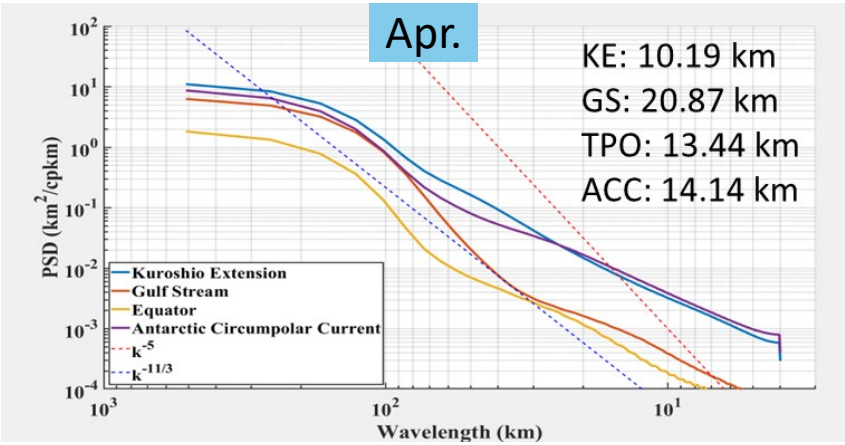
- SWOT: noise level estimated from wavelengths < 15km, spectral slope fitted over 40-125 km.
- Sentinel-6A: noise level estimated from wavelengths < 25km, spectral slope fitted over 70–250 km.

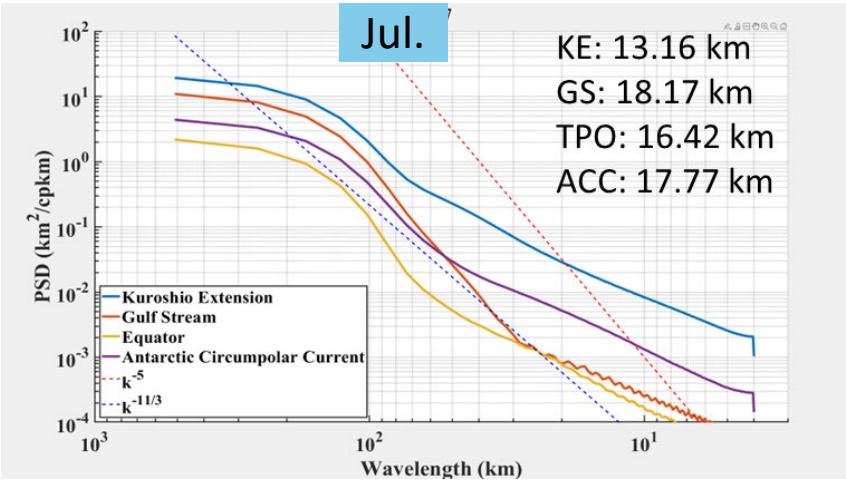


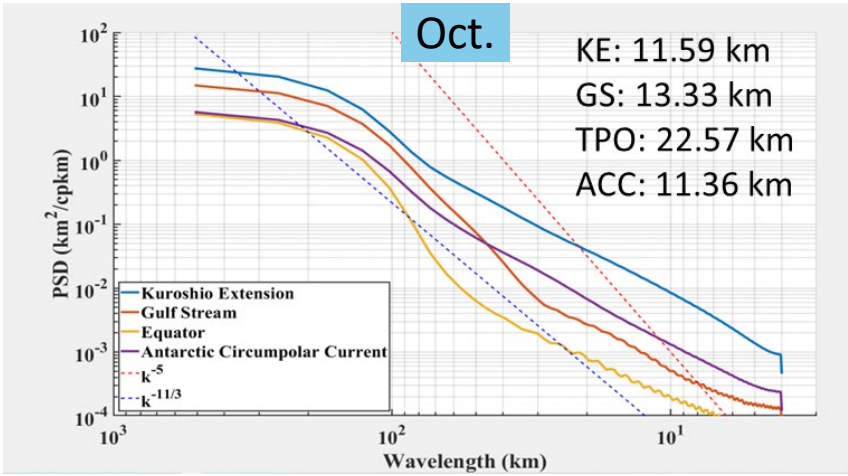
# 1. Evaluation and Analysis of SWOT data

## ➢ PSDs of SWOT in different months



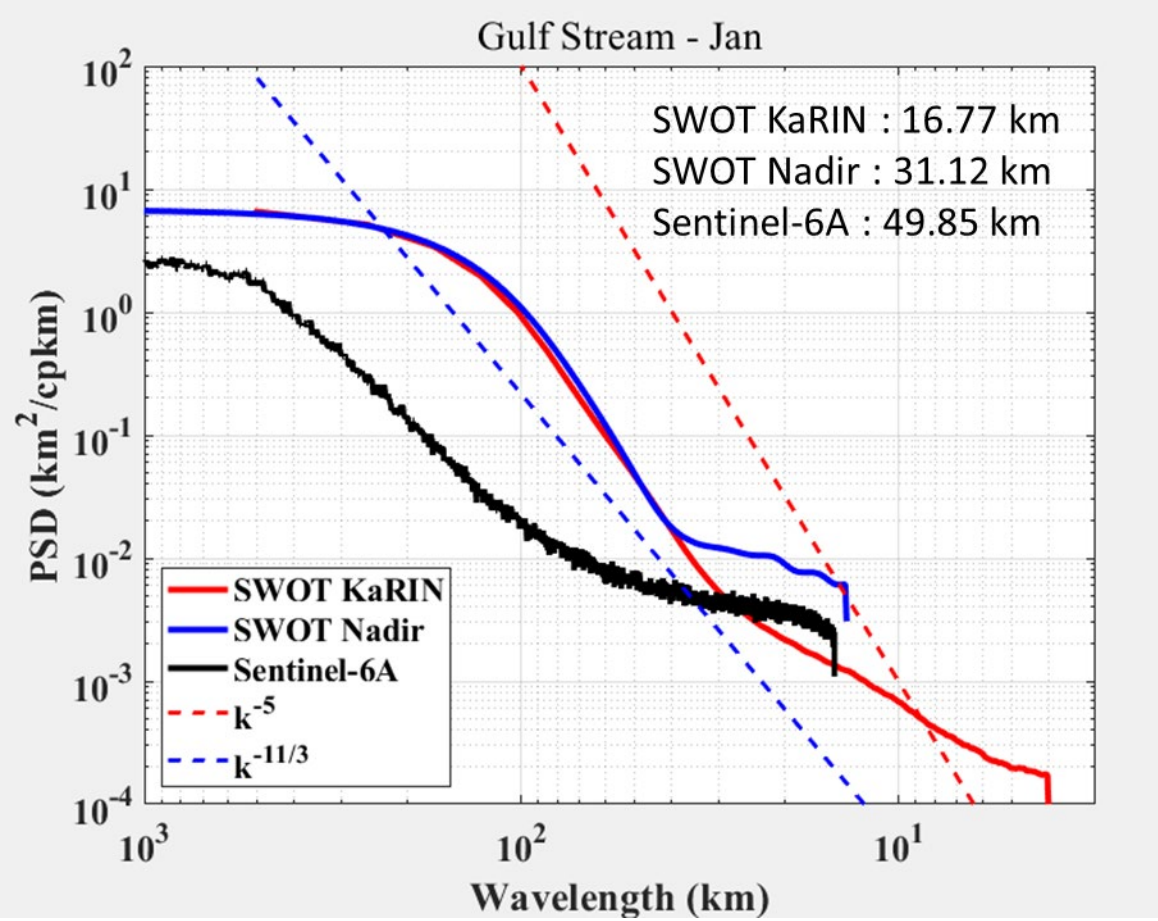



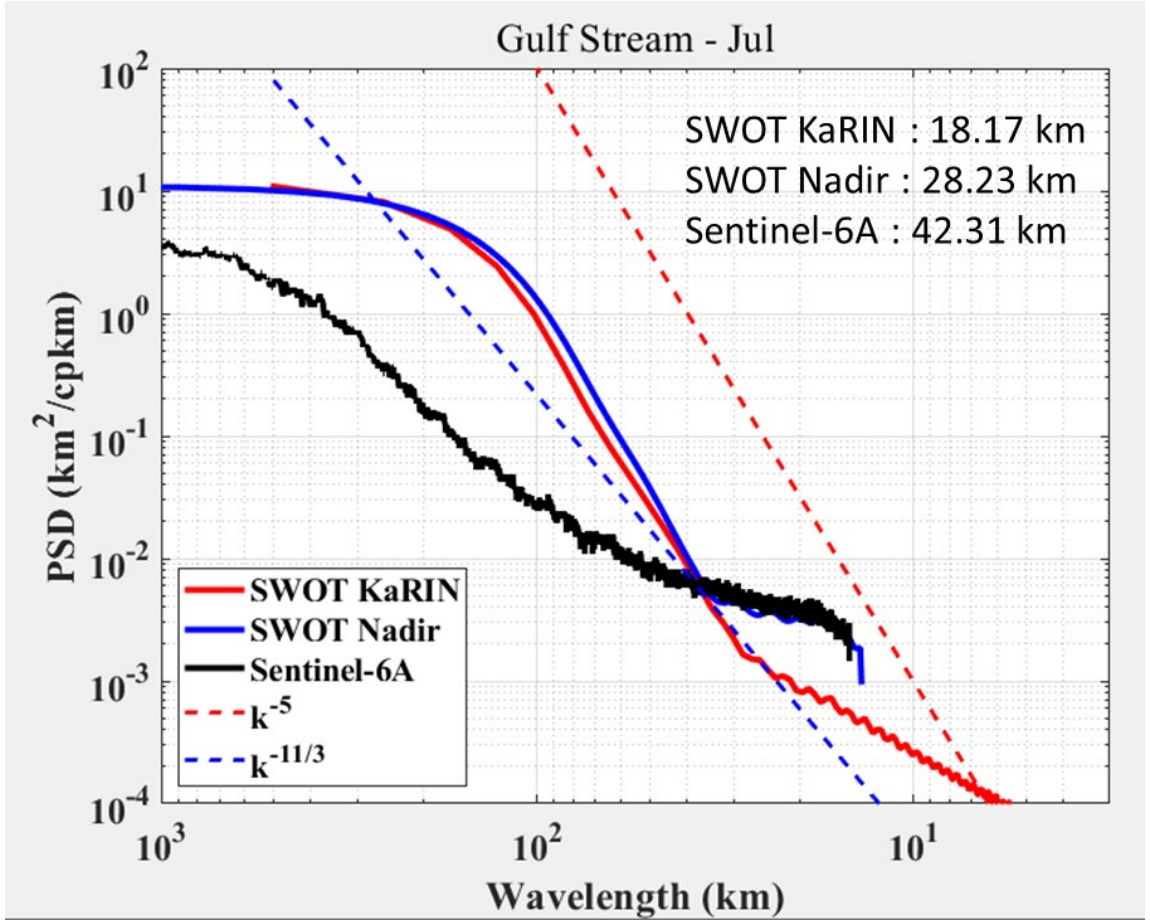




SWOT can capture ocean dynamics down to the minimal wavelength of 10km in KE.

# 1. Evaluation and Analysis of SWOT data

## ➢ Comparisons of the Resolution Capability



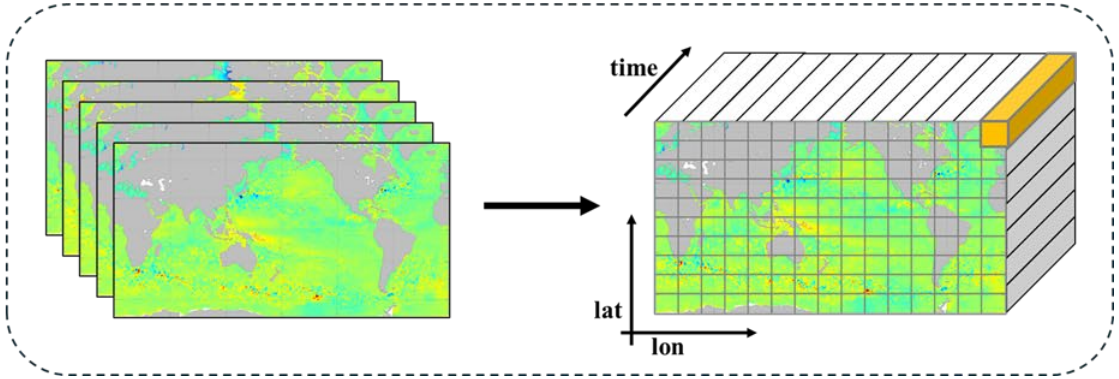

Resolution capability of ocean dynamics by SWOT is greatly better than Sentinel-6.

# 2. Multi-Source Satellite Altimetry Data Fusion

## 2.1 Optimal Interpolation with Adaptive Spatiotemporal Scales

To obtain the adaptive spatiotemporal scales by calculating the global ocean dynamic spatiotemporal correlation scales with high-resolution reanalysis data.

sea surface height data from the ocean reanalysis product

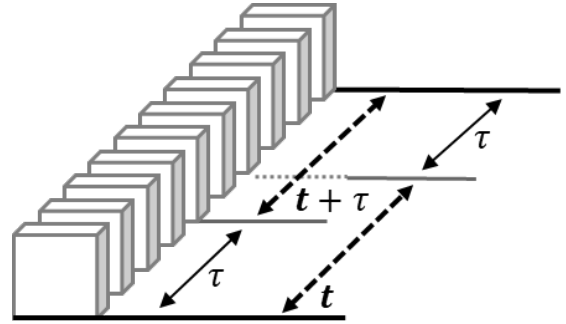



**Spatial Correlation Scale Computation**

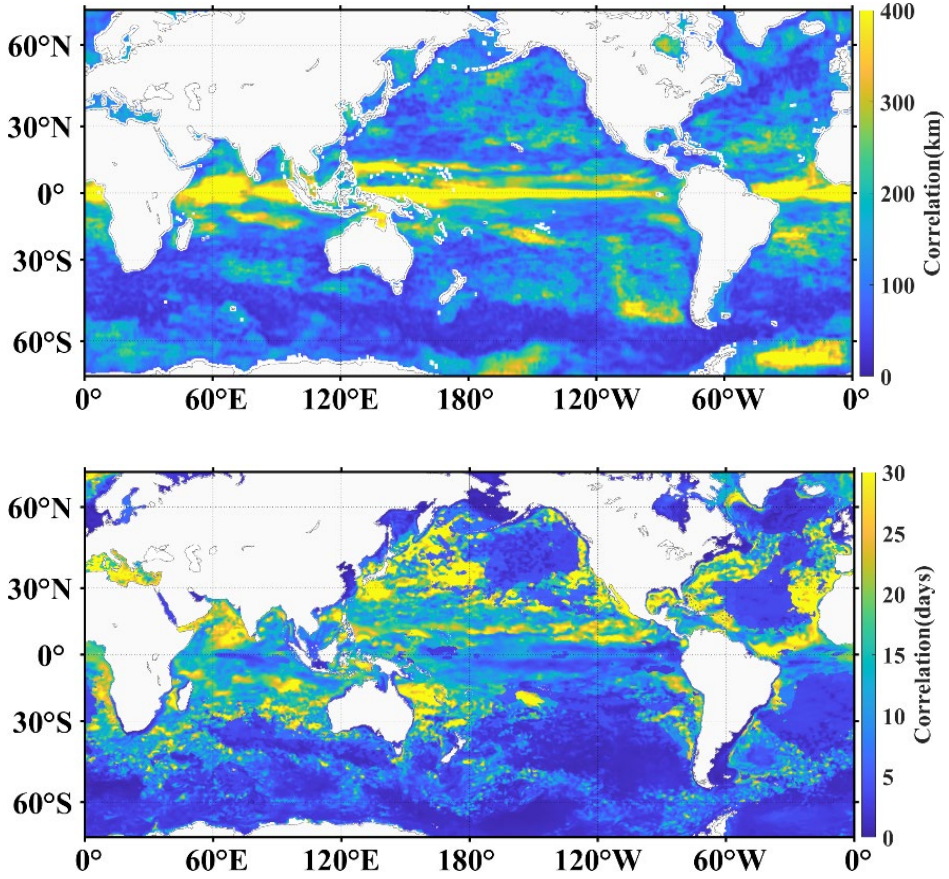
$$\begin{cases} CoL = \dfrac{\sum (X_i - \overline{X_i})(X_{i+n} - \overline{X_{i+n}})}{\sqrt{\sum (X_i - \overline{X_i})^2}\sqrt{\sum (X_{i+n} - \overline{X_{i+n}})^2}} \\ L = \sqrt{(N_1 \cdot dx)^2 + (N_2 \cdot dy)^2} \end{cases}$$

**Temporal Correlation Scale Computation**

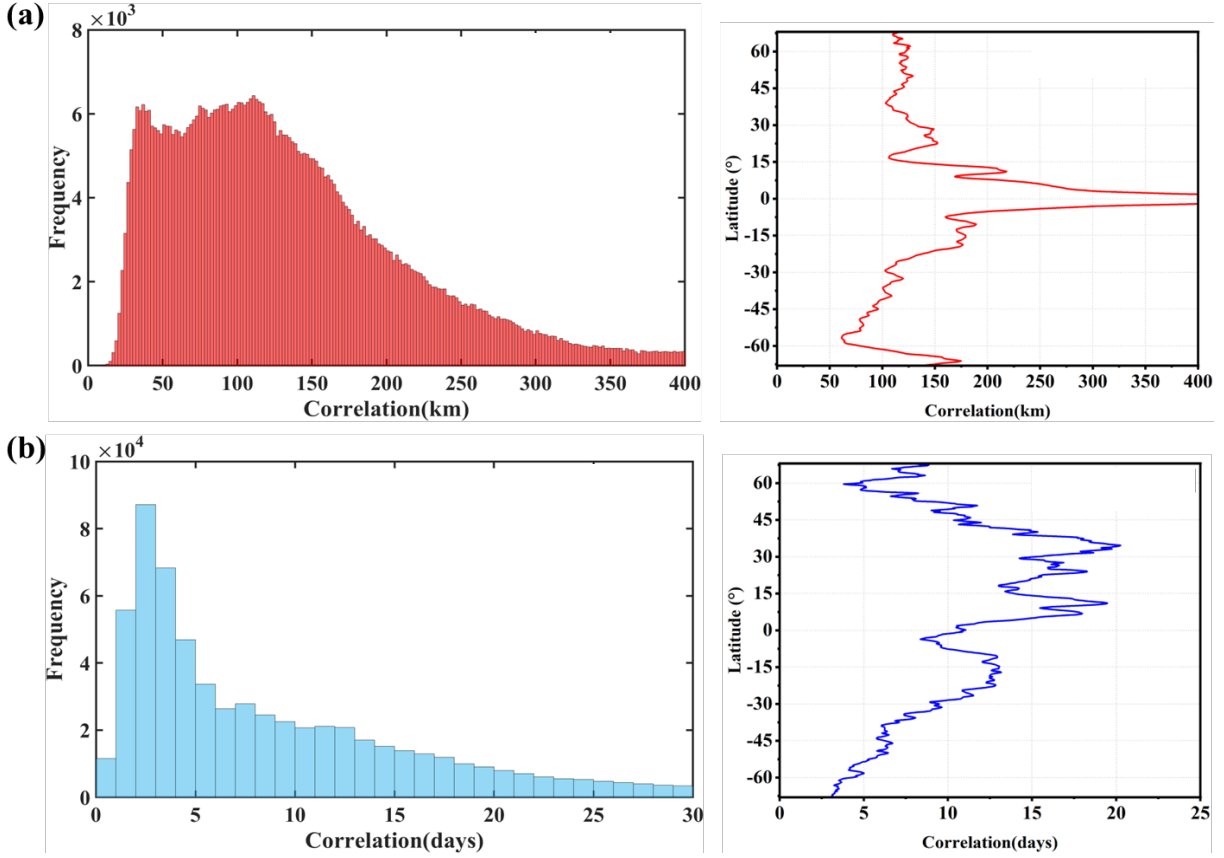
$$\begin{cases} CoT = \dfrac{\sum (X_t - \overline{X})(X_{t+\tau} - \overline{X_{t+\tau}})}{\sqrt{\sum (X_t - \overline{X_t})^2}\sqrt{\sum (X_{t+\tau} - \overline{X_{t+\tau}})^2}} \\ T = \tau_{\max} \end{cases}$$



# 2. Multi-Source Satellite Altimetry Data Fusion




Spatial/Temporal Correlation Scales




Statistical Histograms & Zonal-Mean Distributions

Spatiotemporal correlation scales exhibit latitude-dependent patterns across global ocean dynamics.

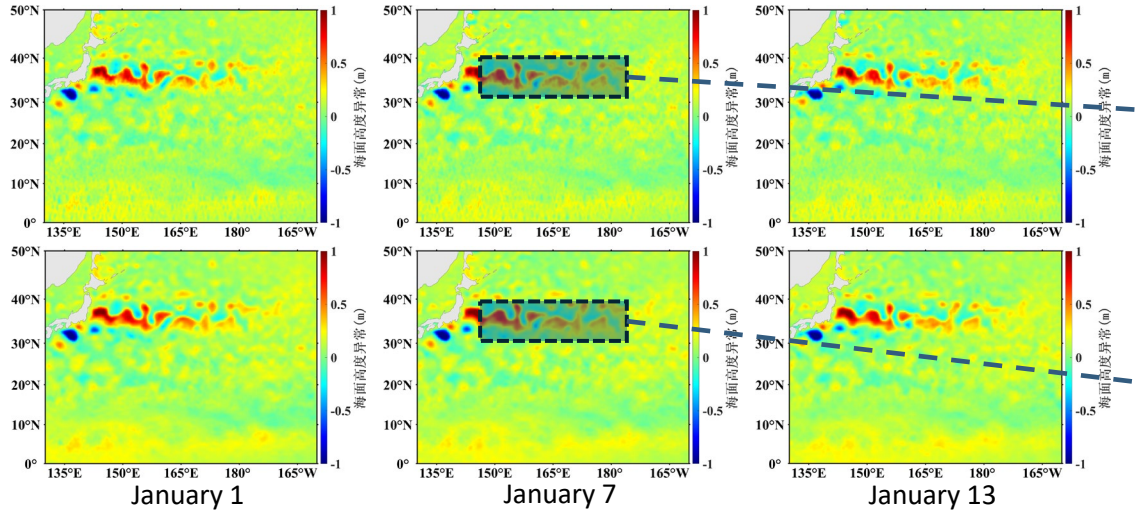
# 2. Multi-Source Satellite Altimetry Data Fusion

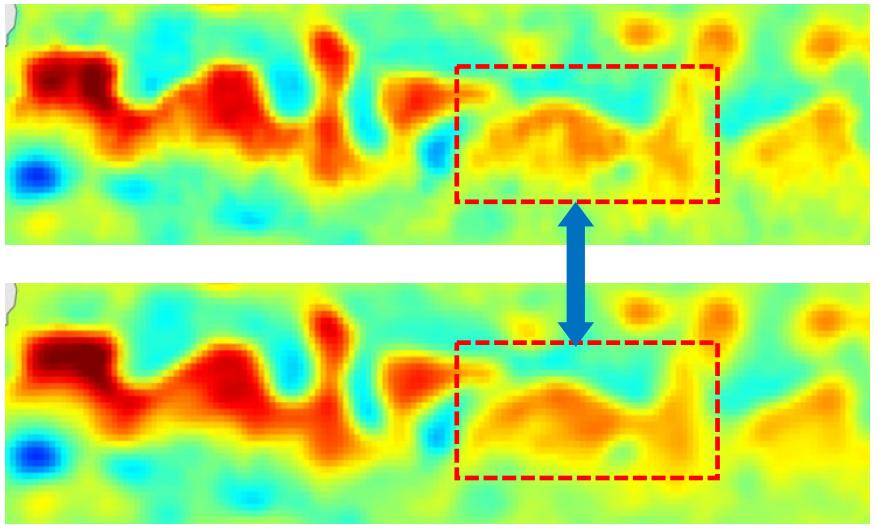
## ➢ Comparison of the fusion results

- **Area:** North Pacific (130°E–160°W, 0°–50°N).
- **Data：** Sentinel-3A/3B, Jason-3, HY-2B during the period of January 1–31, 2023.
- **Method:** Spatiotemporal Optimal Interpolation (OI).
- **Adaptive Scales：** adjustment of spatiotemporal scales based on geographic location.
- **Fixed Scales：** 100 km/10 days.

Fixed:

Adaptive :

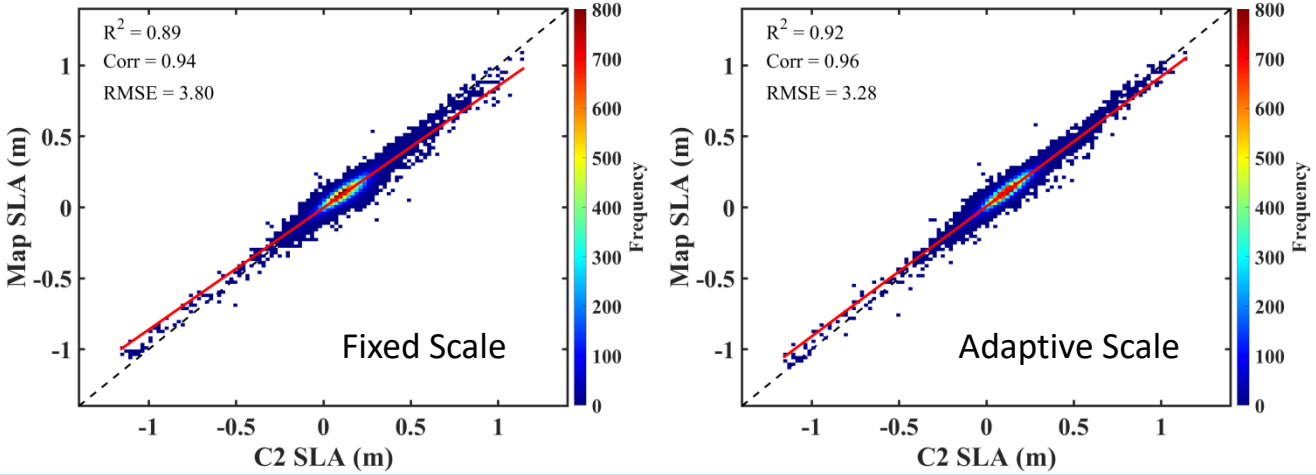


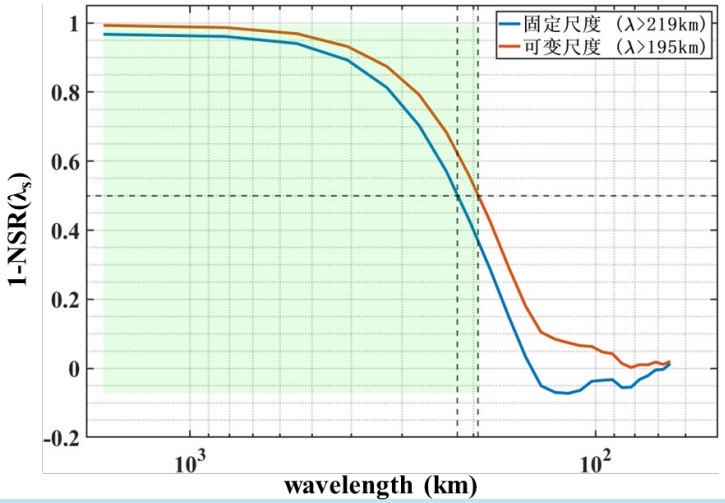



The results of adaptive scales resolve ocean dynamics with more detail information.

# 2. Multi-Source Satellite Altimetry Data Fusion

- **Accuracy Assessment:** Validation by Cryosat-2 along-track data with metrics: Coefficient of Determination($R^2$), Cross-Correlation (Corr) and Root Mean Square Error (RMSE).
- **Effective Resolution Assessment:** The effective resolution is determined by computing the spectral density ratio between fusion errors ($SLA_{C2} - SLA_{map}$) and Cryosat-2 along-track data via Fourier transform. The wavelength where this ratio equals 1/2 defines the effective resolution.




- Adaptive scales demonstrate quantitatively higher accuracy.
- Adaptive scale fusion results retain more small-scale signals and improve the effective resolution.

## 2.2 Two-Dimensional Variational Method (2D-Var)

The analysis field ($x^a$) is calculated using the observational data ($y^o$) and the background field ($x^b$), and weighted with background error (B) and observation error (R) to determine the optimal solution.

$$J(x)=\frac{1}{2}\left(x-x^b\right)^T B^{-1}\left(x-x^b\right)+\frac{1}{2}\left(y^o-Hx\right)^T R^{-1}\left(y^o-Hx\right) \Longrightarrow x^a=x^b+\left(B^{-1}+H^T R^{-1} H\right)^{-1} H^T R^{-1}\left(y^o-Hx^b\right)$$

- **Background Error Covariance Matrix (B):**

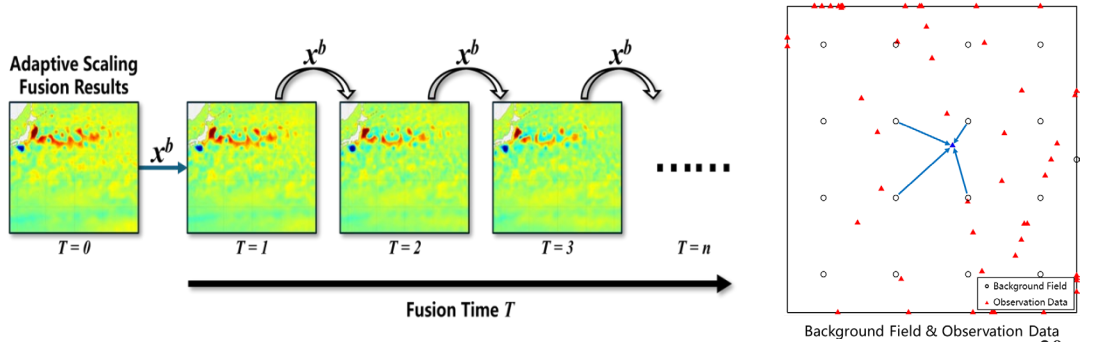
$$B=\Sigma C \Sigma$$

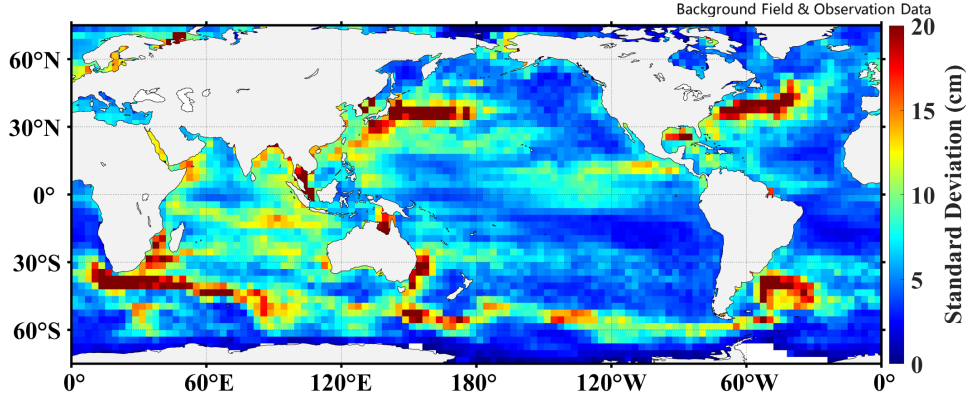
$\Sigma$ represents the root mean square estimate of the background error, and C is the spatial correlation matrix.

- **Observation Error Covariance Matrix (R):**

$$R=R^m+R^t$$

- $R^m$: **Instrumental errors** from measurement imperfections.
- $R^r$: **Representativeness errors** due to temporal sampling inconsistencies.

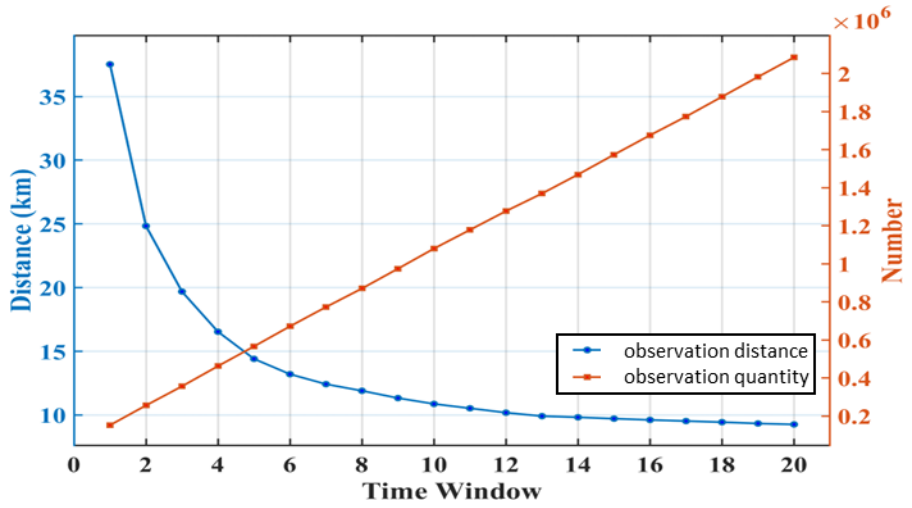


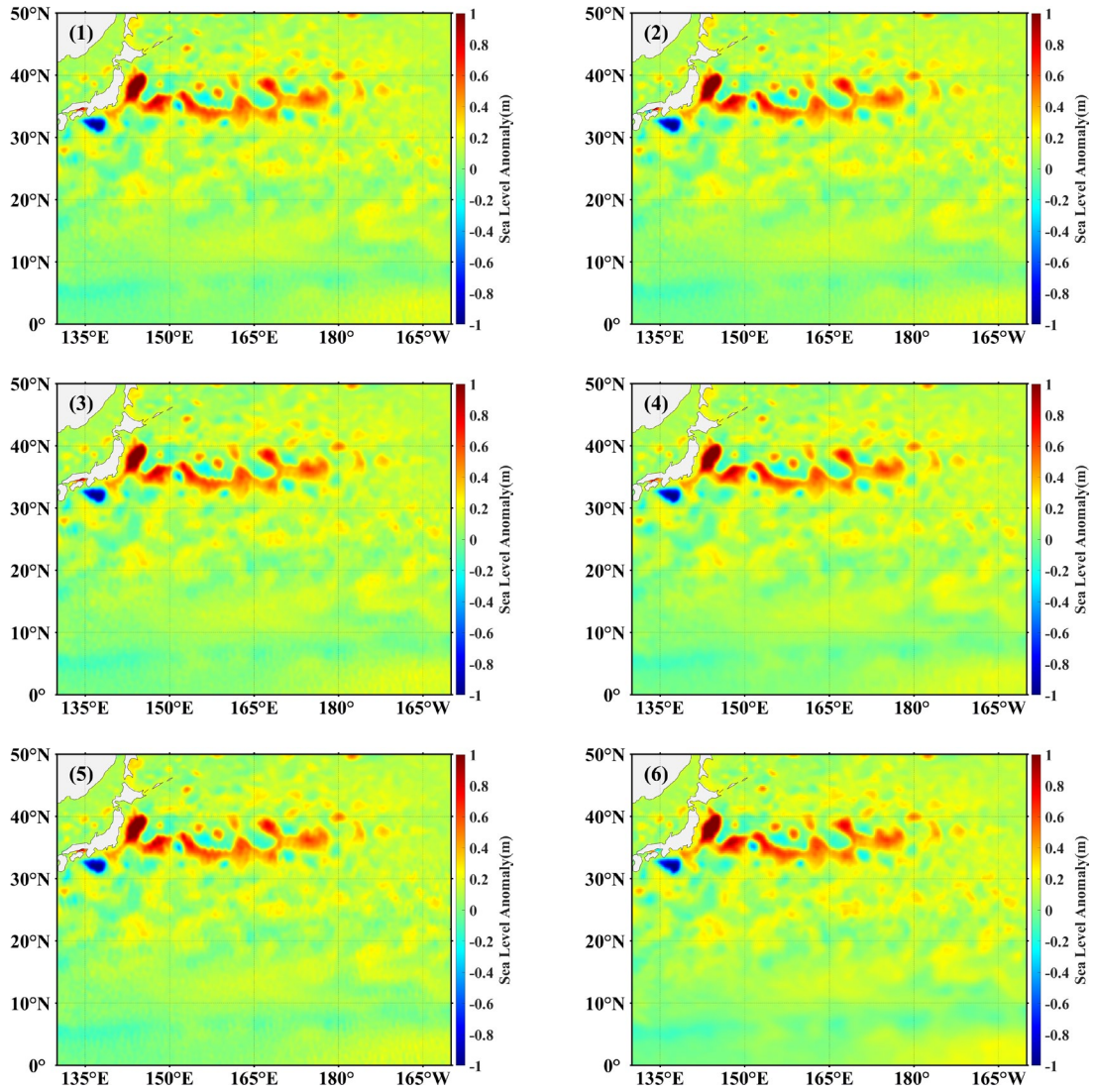
# 2. Multi-Source Satellite Altimetry Data Fusion

## ➢ 2D-Var Fusion Experiment

| ID | Time Window | Scale L | $x^b$ | $R^t$ |
|---|---|---|---|---|
| **Case1** | ±12 days | 65 km | Prior Fusion Field | Used |
| **Case2** | ±20 days | 65 km | Prior Fusion Field | Used |
| **Case3** | ±12 days | 65 km | Smoothed Field | Used |
| **Case4** | ±12 days | 100 km | Prior Fusion Field | Used |
| **Case5** | ±12 days | 65 km | Prior Fusion Field | Not Used |



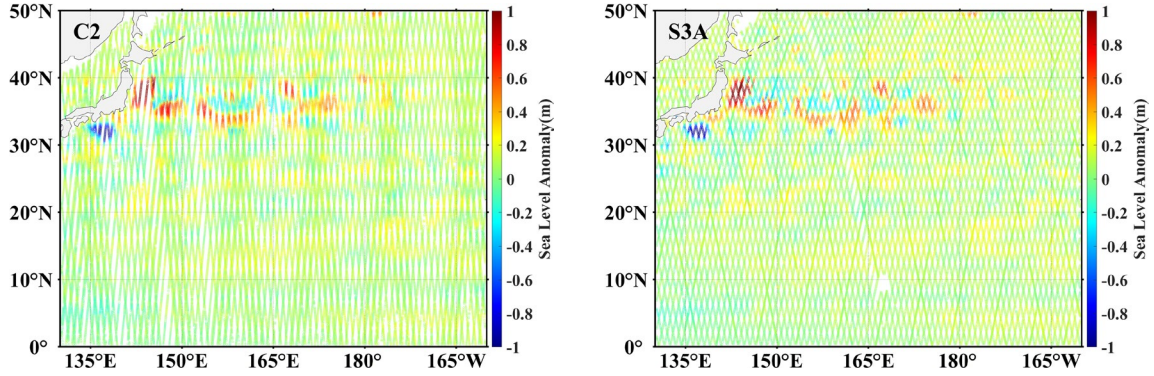

Number of Observation & Mean Minimum Observation Distance (km)



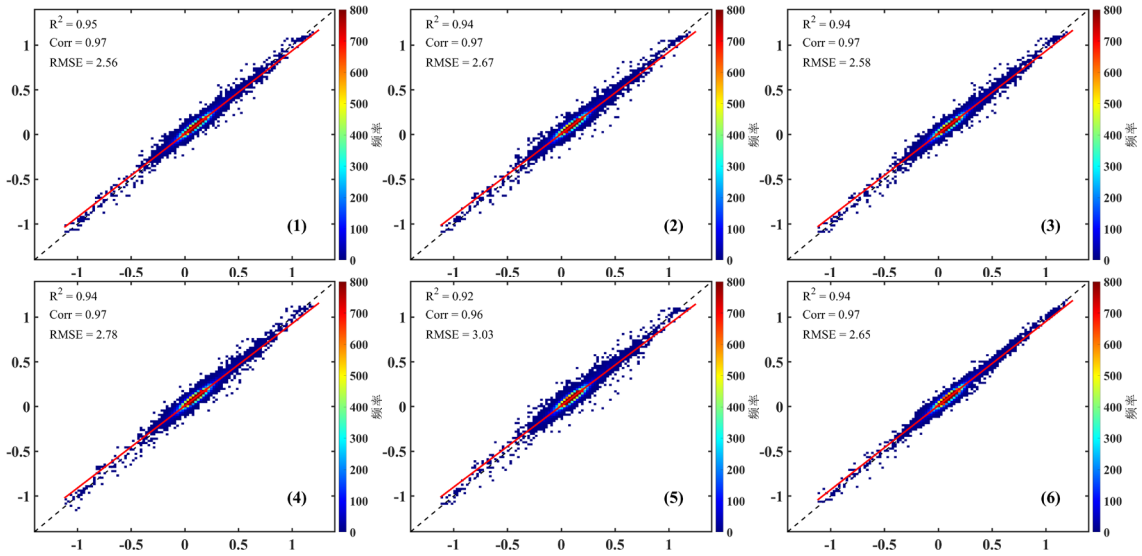
# 2. Multi-Source Satellite Altimetry Data Fusion

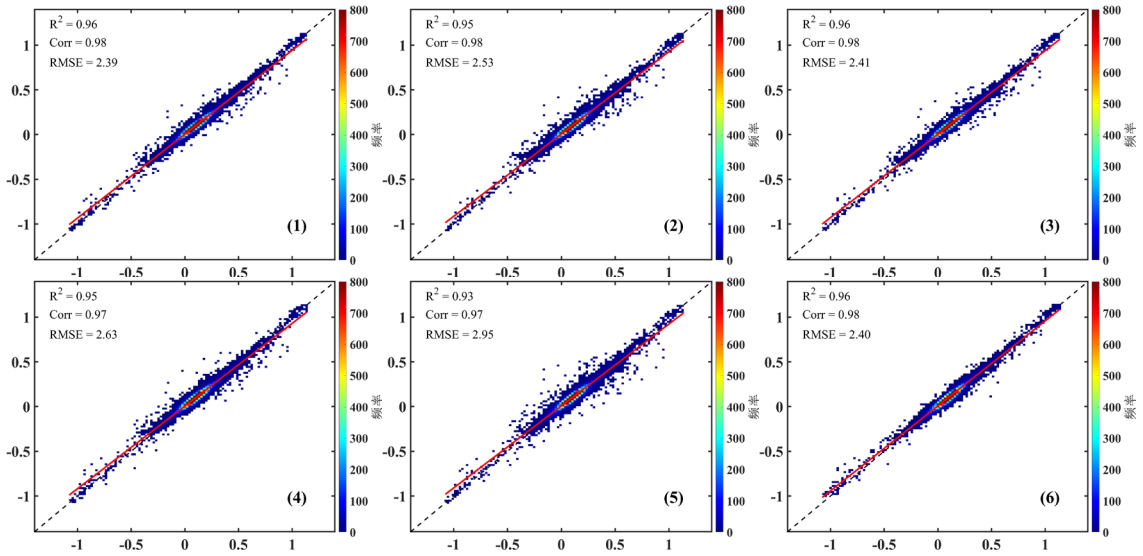
## ➢ Accuracy Assessment

The contemporaneous **Cryosat-2 (C2)** and **Sentinel-3A (S3A)** along-track data are used in accuracy assessment.




Along-track data of C2 and S3A



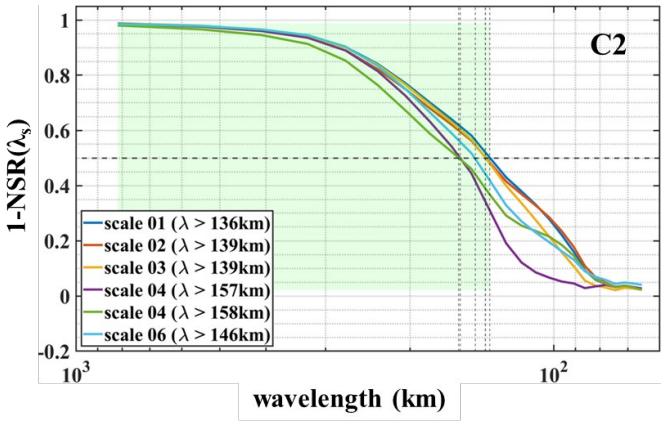



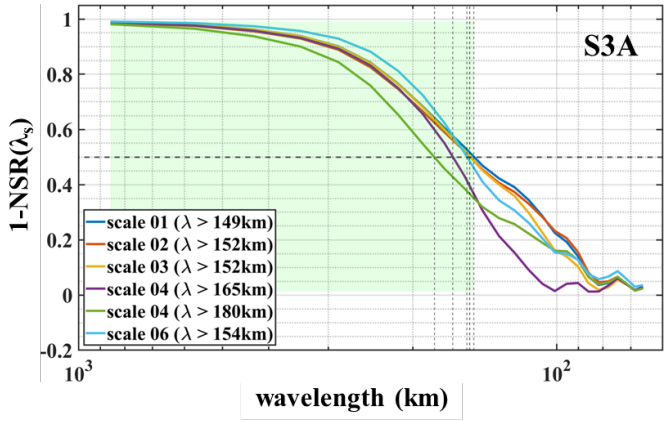

Scatter plot of comparisons between fusion results and C2/ S3A

Case1 has the best fusion accuracy, and its RMSE is 2.475 cm.

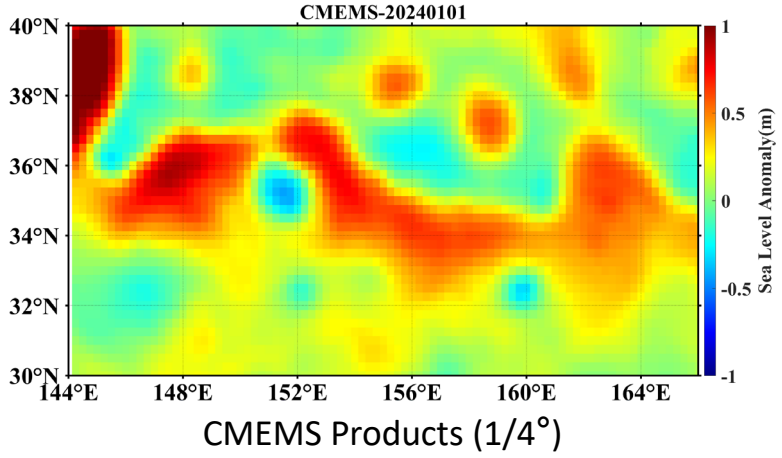
# 2. Multi-Source Satellite Altimetry Data Fusion

➢ **Comparison of effective resolution between fusion results and CMEMS products**

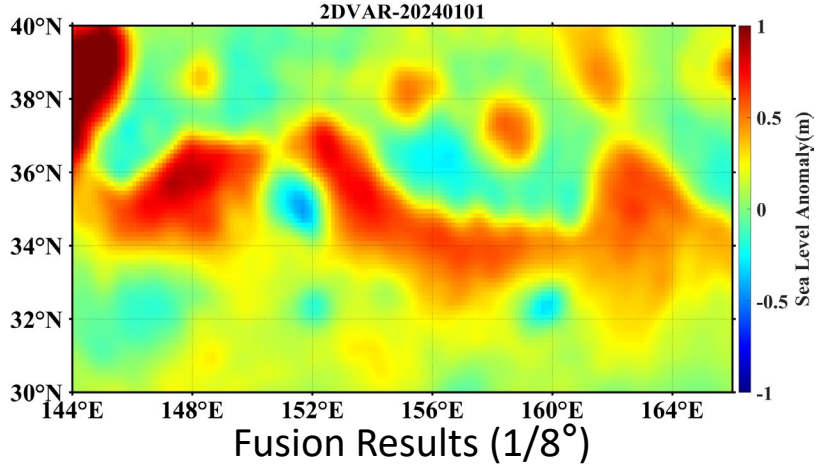



➢ The average effective resolution of the CMEMS product is about 150 km, and 2-D variational fusion result is **142 km**.




CMEMS Products (1/4°)




Fusion Results (1/8°)

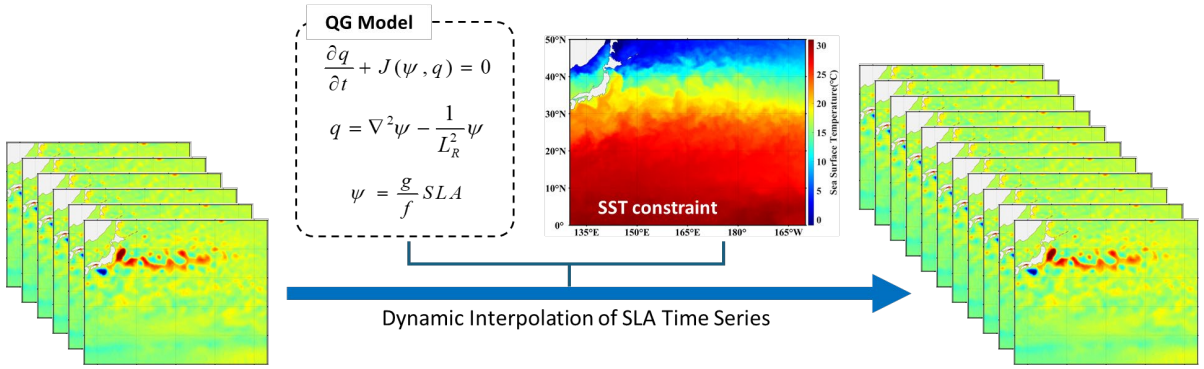
**The resolution is improved and more information about the sea surface height is retained**

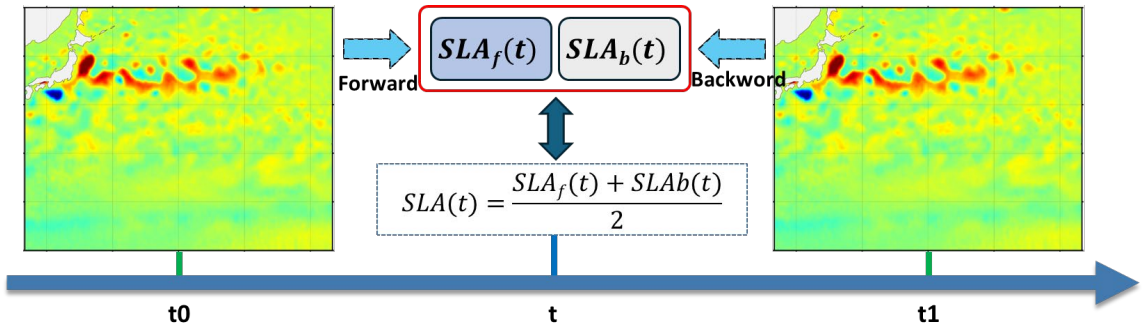
The 2D-var fusion method can retain more observation information and improve the parsing ability of SLA variabilities.

# 2. Multi-Source Satellite Altimetry Data Fusion

## 2.3 Dynamic Interpolation of SLA Time Series

A quasi-geostrophic (QG) model and SST data is introduced as a physical constraint to SLA time series interpolation and the temporal resolution of the SSH fusion product is improved.



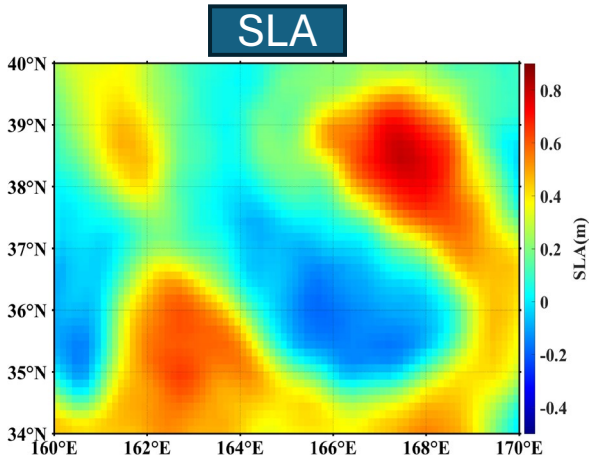



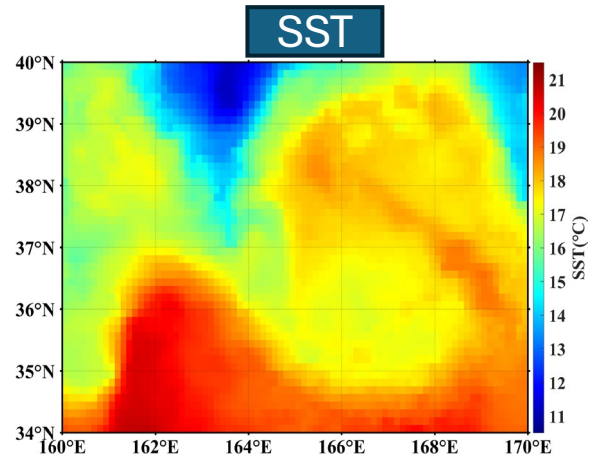

- Calculate the initial Potential Vorticity (PV) $q_0$ using SLA.
- Update flow field vector U=(u, v) by SST constraint.
- Update the PV $q$ over time using the horizontal flow field vector U=(u, v).
- Calculate the new flow function ψ by the updated PV $q$.
- Calculate the time updated SLA by new flow function.
- Obtain the dynamic interpolation result by average the forward and backward results.

# 2. Multi-Source Satellite Altimetry Data Fusion

## Update flow field vector by SST constraint

- High resolution SST data contains information on small-scale ocean dynamic processes, and provides more refined information.
- High resolution SST can compensate for the shortcomings of SLA data in analyzing small-scale ocean processes.
- Update the flow field vector based on geostrophic current calculation by SLA and the spatial and temporal gradient of SST data.



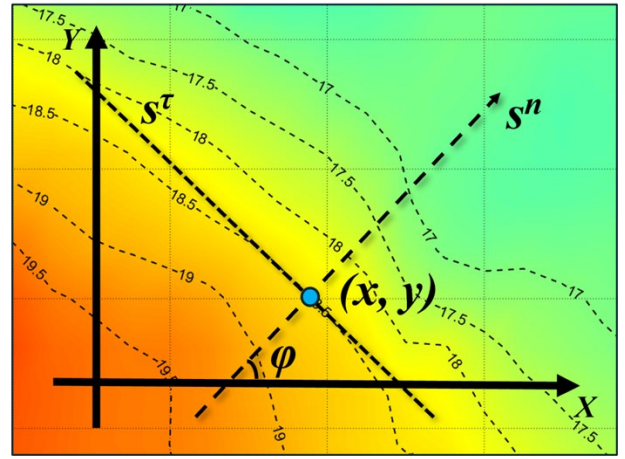




$$F = \frac{\partial SST}{\partial t} + u\frac{\partial SST}{\partial x} + v\frac{\partial SST}{\partial y}$$

$$-h < \frac{\partial SST}{\partial t} + u\frac{\partial SST}{\partial x} + v\frac{\partial SST}{\partial y} - F_{bck} < h$$

$$\begin{cases} u = s^{\tau}\cos\varphi - s^{n}\sin\varphi \\ v = s^{\tau}\sin\varphi + s^{n}\cos\varphi \end{cases} \qquad \begin{cases} s^{\tau} = u\cos\varphi + v\sin\varphi \\ s^{n} = -u\sin\varphi + v\cos\varphi \end{cases}$$

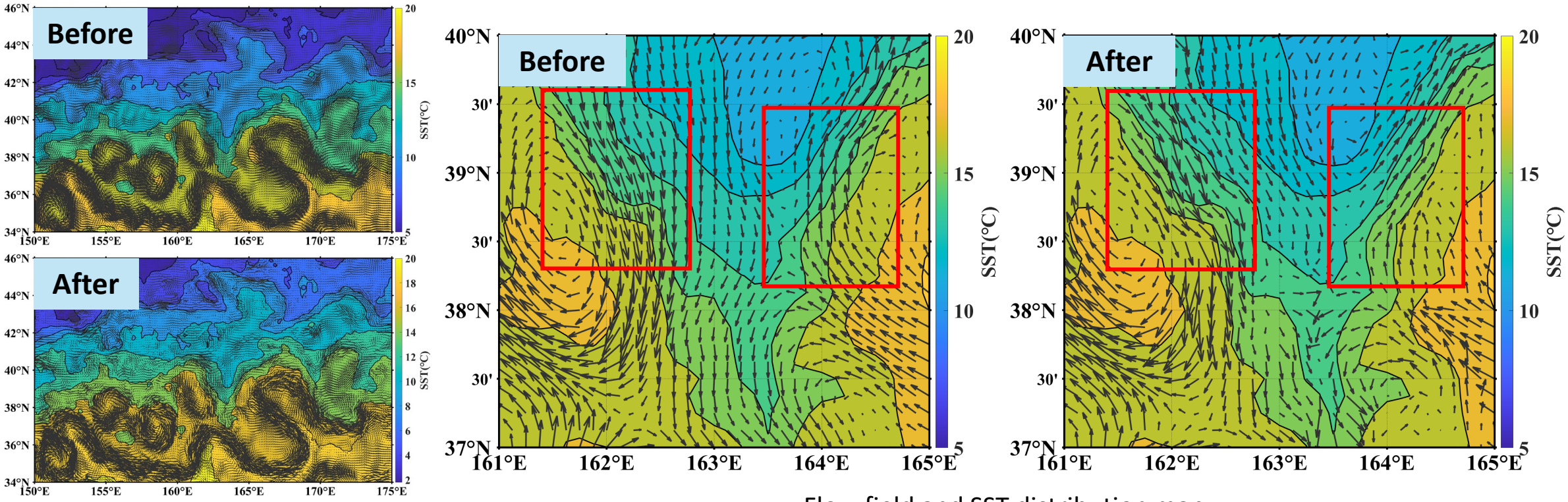
$$U = \begin{cases} u = u_g - \dfrac{A(Au_g + Bv_g + E)}{A^2 + B^2} \\ v = v_g - \dfrac{B(Au_g + Bv_g + E)}{A^2 + B^2} \end{cases}$$




Velocity vector decomposition (dashed lines represent tangential component $s^{\tau}$ and normal component $s^{n}$ at (x, y) )

# 2. Multi-Source Satellite Altimetry Data Fusion

## Flow field before and after correction



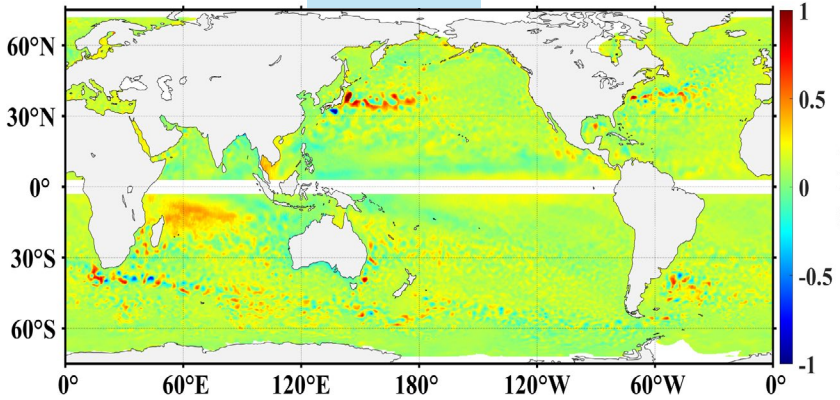

Flow field and SST distribution map

The flow velocity vector before correction has obvious unreasonable distribution in some areas, and some flow vectors directly cross the isotherm, which is inconsistent with the physical characteristics of real seawater flow and fails to accurately reflect the characteristics of seawater flow along the isotherm.

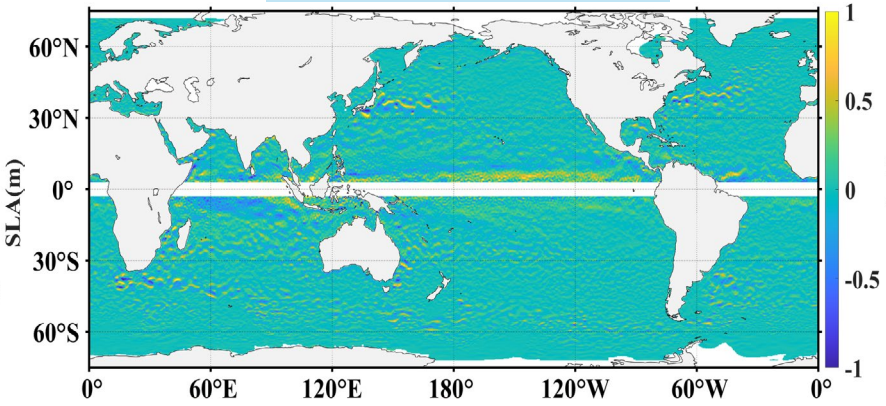
# 2. Multi-Source Satellite Altimetry Data Fusion

CSTEC 中国科学技术交流中心 China Science and Technology Exchange Center
esa → THE EUROPEAN SPACE AGENCY

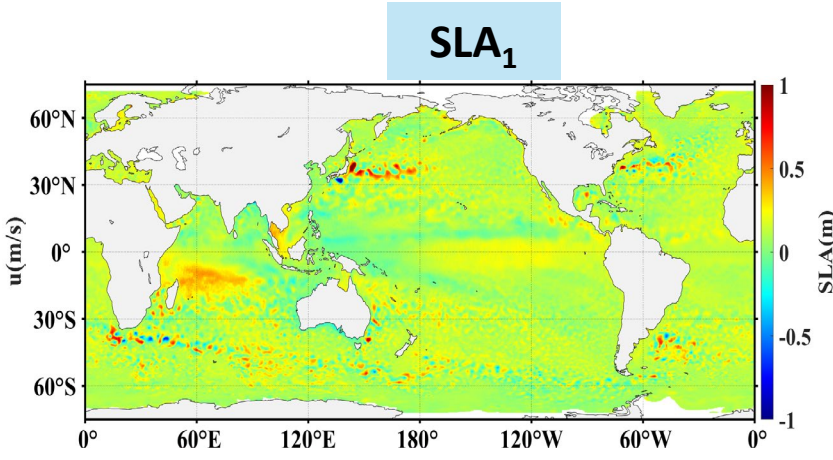
**$SLA_0$**



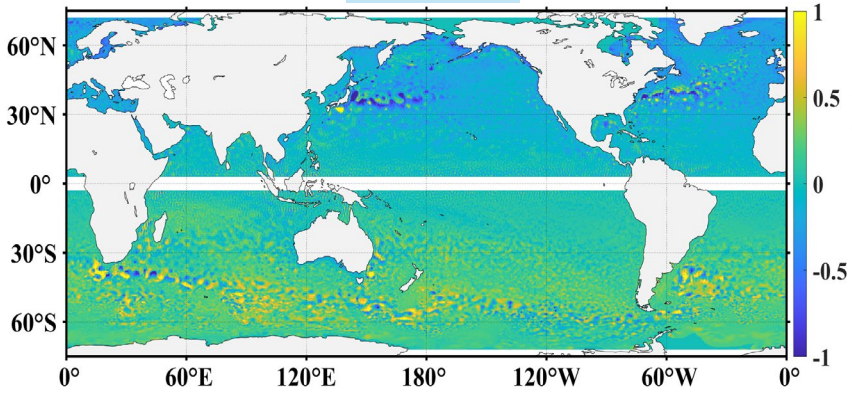

**Flow vector - U**



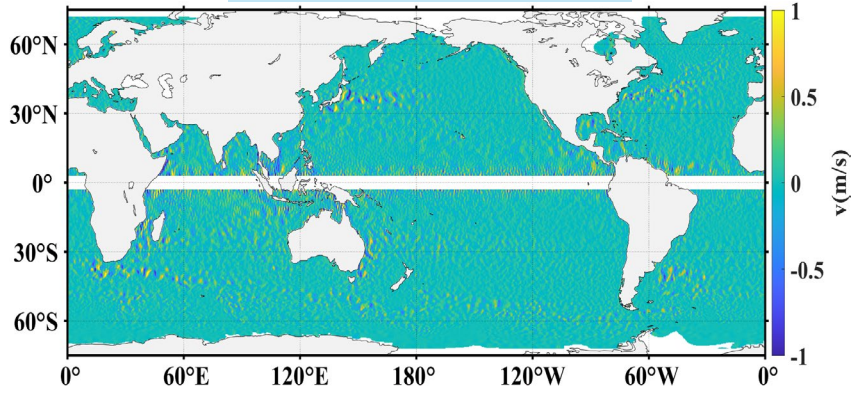

**$SLA_1$**

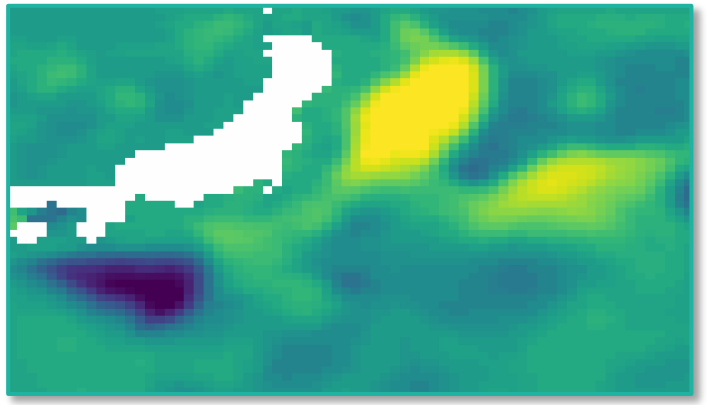



**PV**




**Flow vector - V**



The temporal evolution of SLA

# 3. Submesoscale SSH Mapping along the East Greenland Coast

## Dynamic mapping Model of SWOT SSH

- Mapping small-scale SSH from SWOT Using a dynamical optimal interpolation approach by Introducing QG physics.
- 1-layer QG model capturing first baroclinic mode.
- Assimilate altimetry data via Back and Forth Nudging (BFN).
- Boundary and initial conditions from DUACS gridded SSH.

QG model based on conservation of potential vorticity, $q$ :

$$\frac{\partial q}{\partial t} + J(\psi, q) = 0, \quad q = \nabla^2\psi + \frac{1}{L_R^2}\psi \longrightarrow \psi = \frac{g}{f}\mathrm{ADT}$$

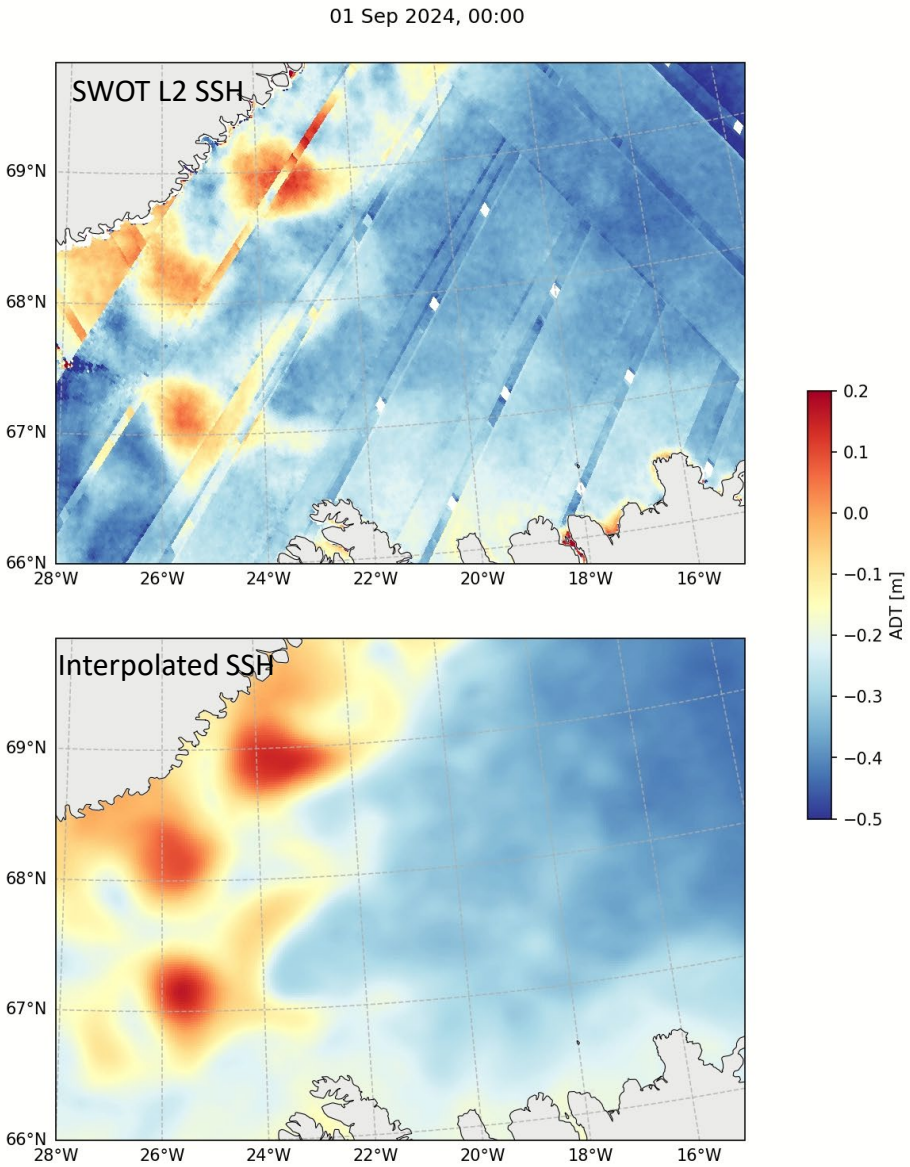
Geostrophic streamfuntion $\psi$ is related to altimetry observations, Absotute Dynamic Topography (ADT)

Forward nudging:

$$\frac{\partial q}{\partial t} = (q,t) + K\left(q^{obs} - q\right), \qquad 0 \le t \le T$$
$$q(t) = q_0$$

Backward nudging:

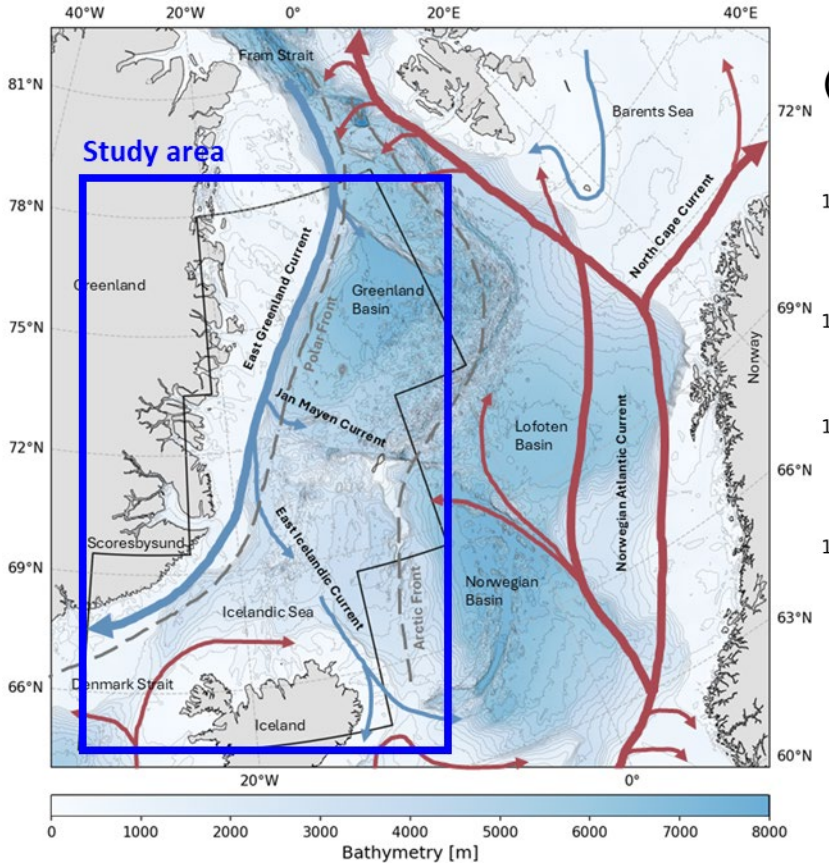
$$\frac{\partial q}{\partial t} = (q,t) - K\left(q^{obs} - q\right), \qquad T \ge t \ge 0$$
$$q(t) = q_T$$

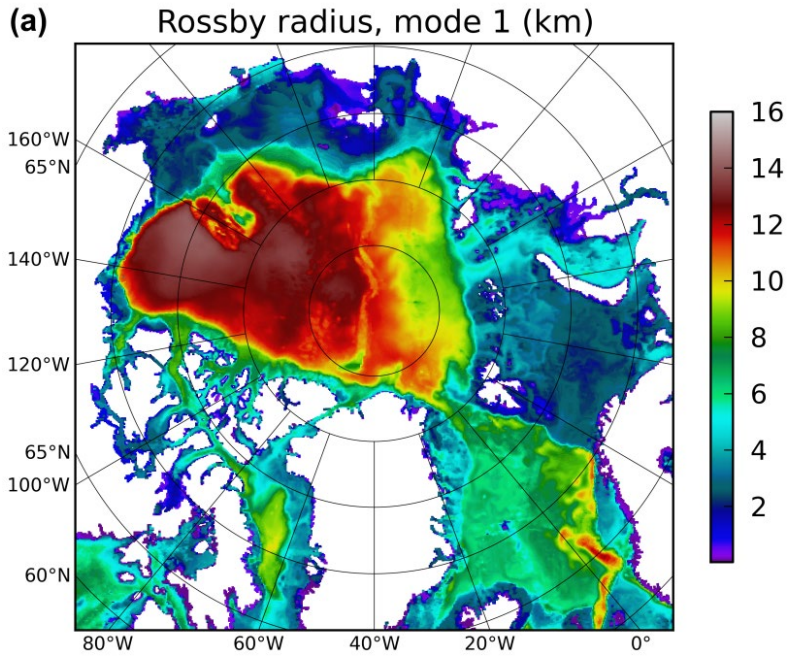


# East Greenland Shelf

A challenging area:

- Coastal and shelf dynamics might not be fully described by QG physics.
- First baroclinic radii is very low (the characteristic horizontal scale of mesoscale processes).
- Lower SSH variability than that of this method applied before (Gulf stream, Agulhas current).
- Sea ice is present on the shelf October-June.




Nurser, A. J. G. and Bacon, S.: The Rossby radius in the Arctic Ocean, Ocean Sci., 10, 967–975

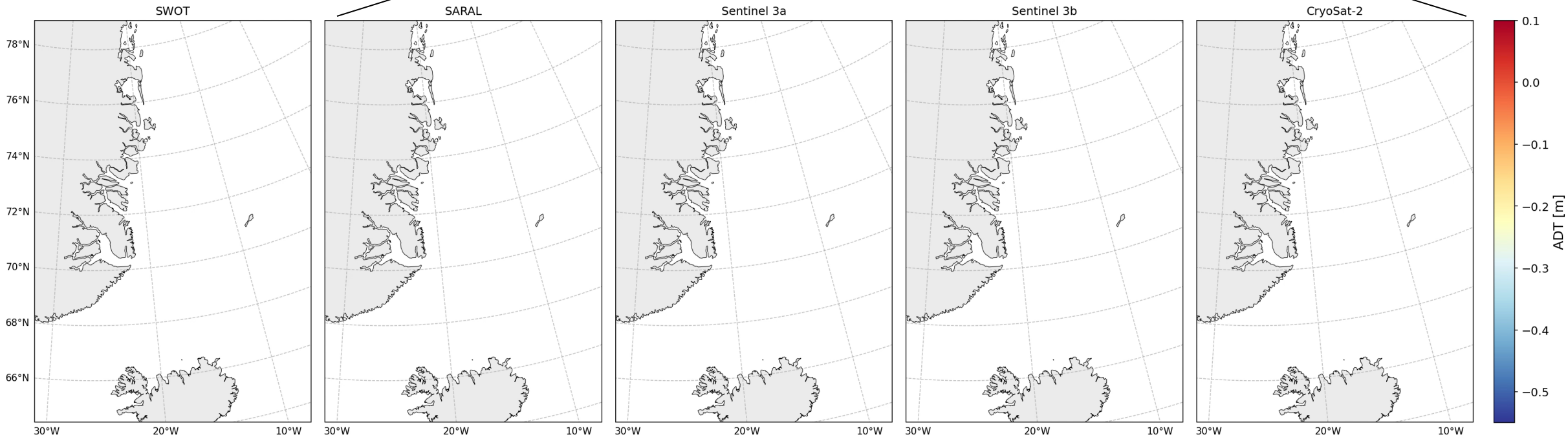
# Altimetry data

SWOT LR L2 science phase

- 2 km resolution

DUACS L3 nadir altimetry

- Quality control and homogenized
- unfiltered

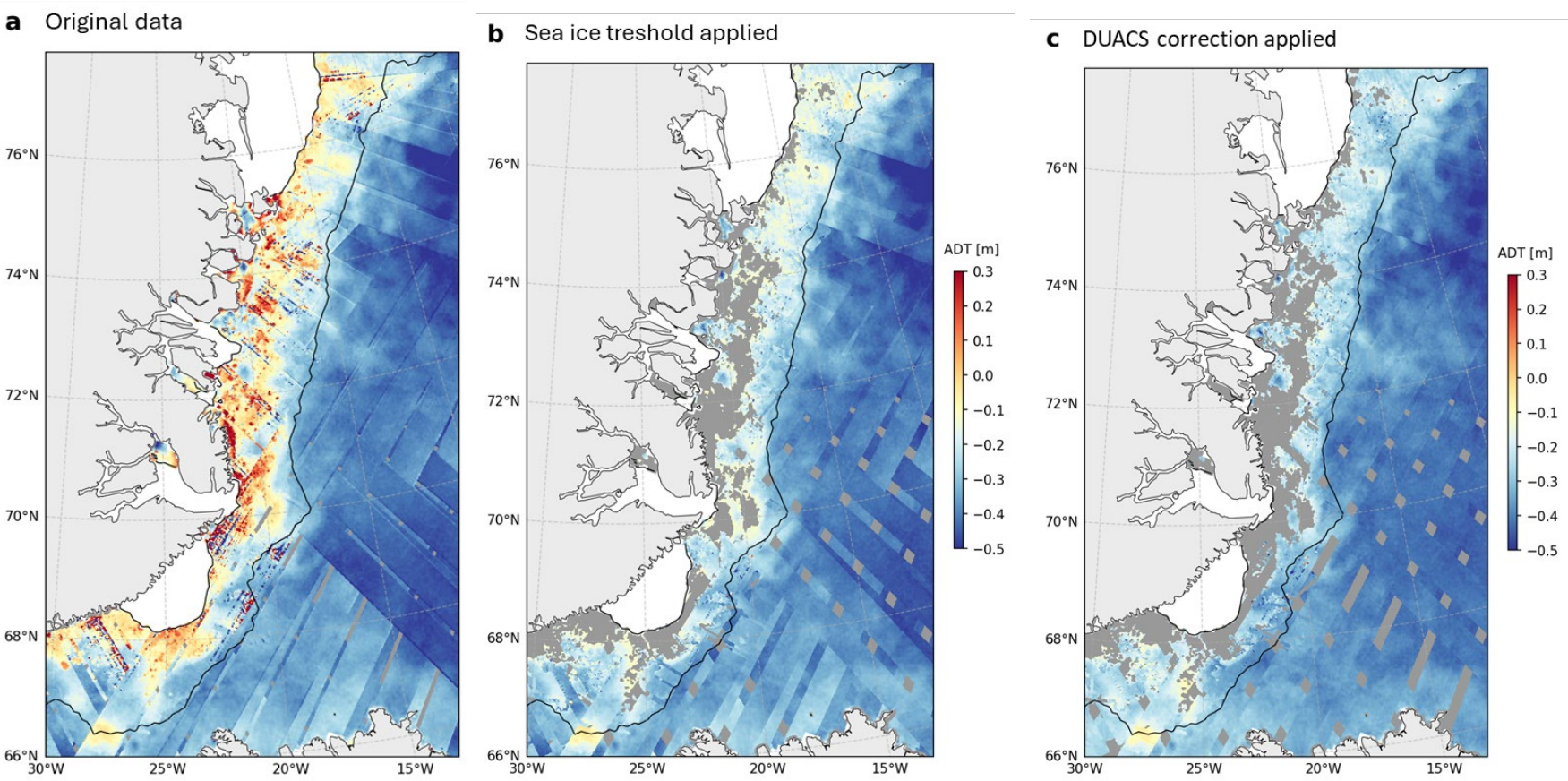



20 Aug 2024, 00:00

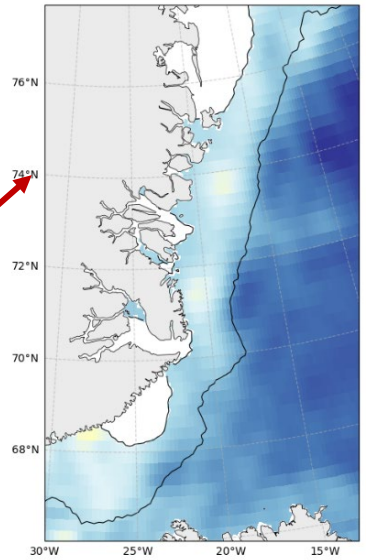
**10 days of observations**

# Removing Sea ice

- Sea ice present on the shelf 9 months of the year.
- Sea ice floes removed using a threshold (-0.1 m).
- Increase the amount of data in sea ice zone (better than using OSI-SAF ice mask).
- Some quality flags are applied.




10 days of data, June 10th to 20th, 2024, Black line is 5% sea ice concentration contour from OSI-SAF on June 15th




Long wavelength signal in SWOT (>50 km) fitted to DUACS

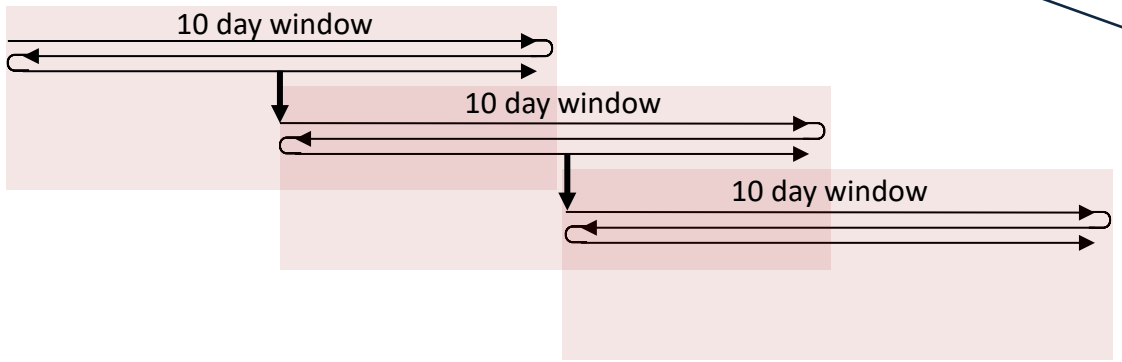
# Homogenization

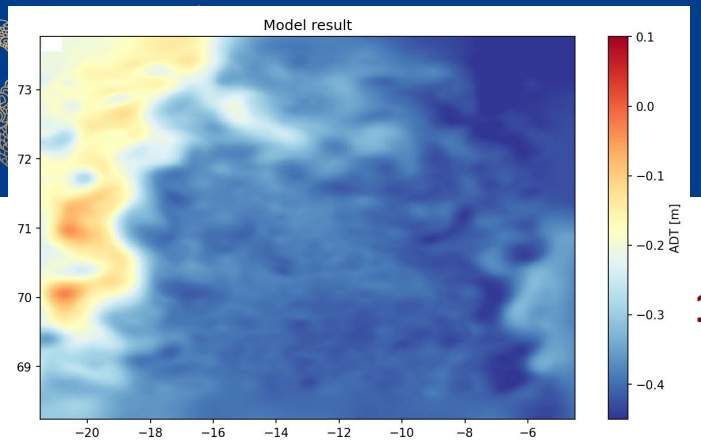
- Remove left over correlated errors.
- Ensure homogenization with DUACS (nadir data and boundary conditions).

# Assimilation

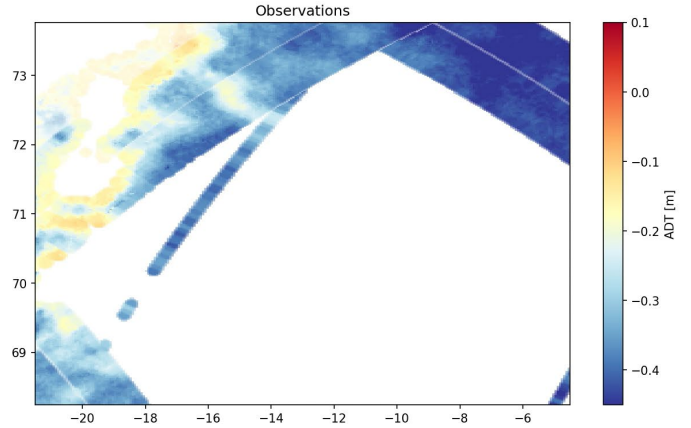
- BFN assimilation performed in windows of 10 days.
- 2 km resolution and 3-hour temporal resolution.
- Nadir altimetry data helps constrain model where SWOT is not available.
- Nudging coefficient with exponential decay in time and space

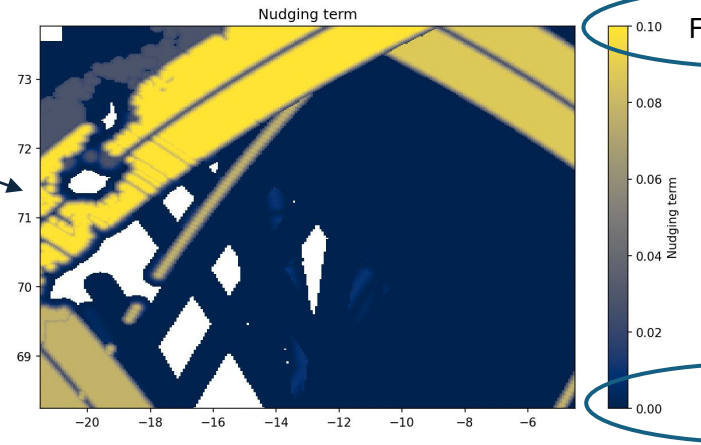
$$\frac{\partial q}{\partial t} = (q,t) + K\left(q^{obs} - q\right)$$




1 month run

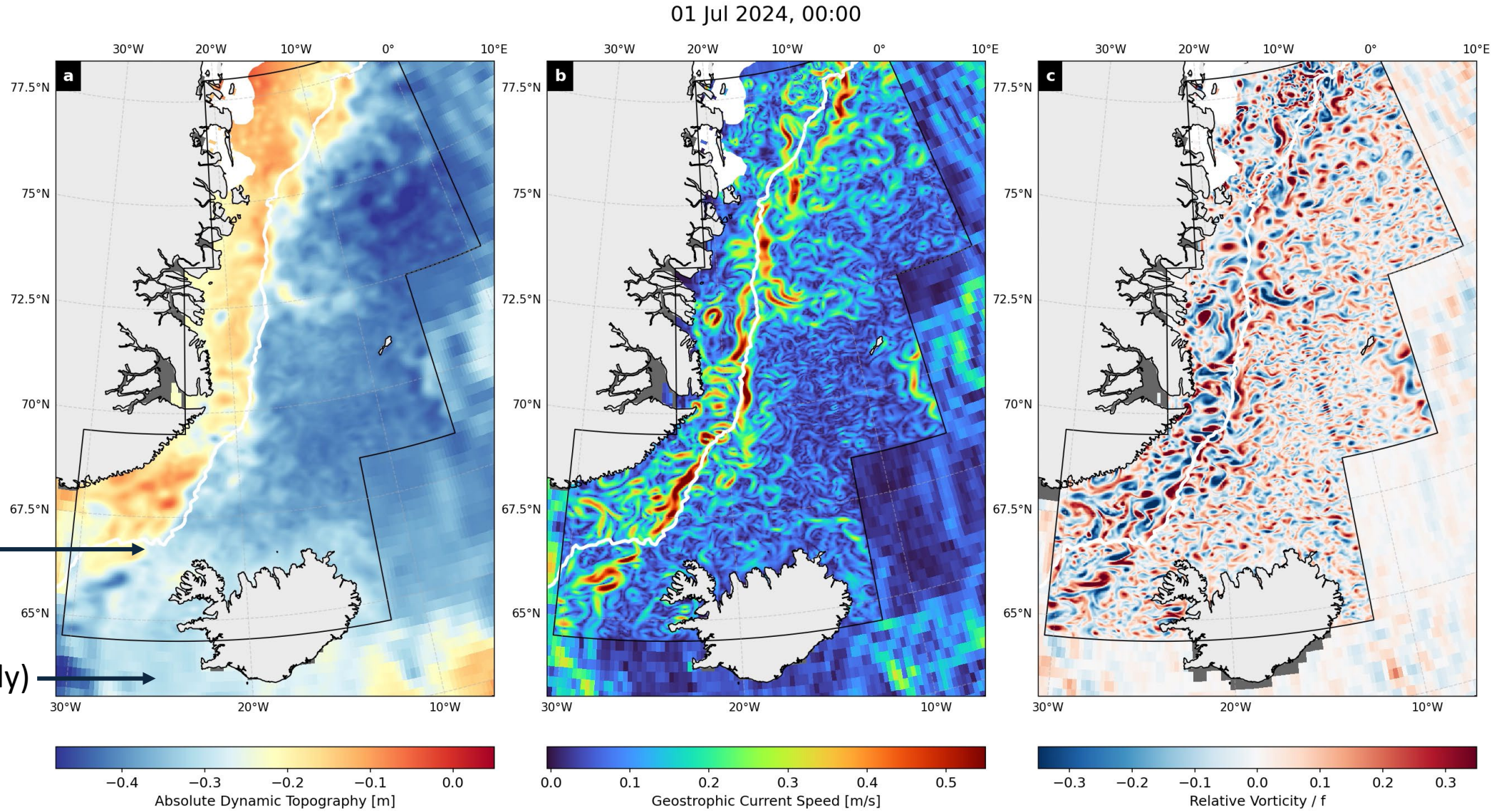



Full weight

Observation weights

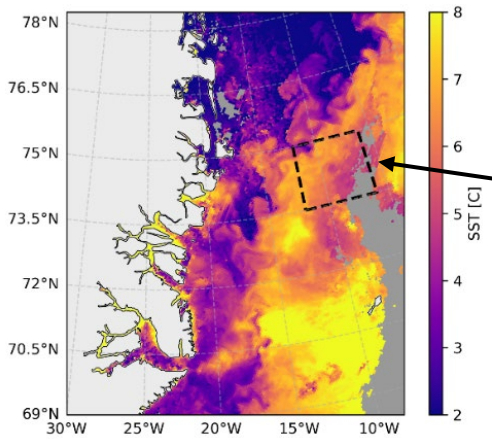
Not used



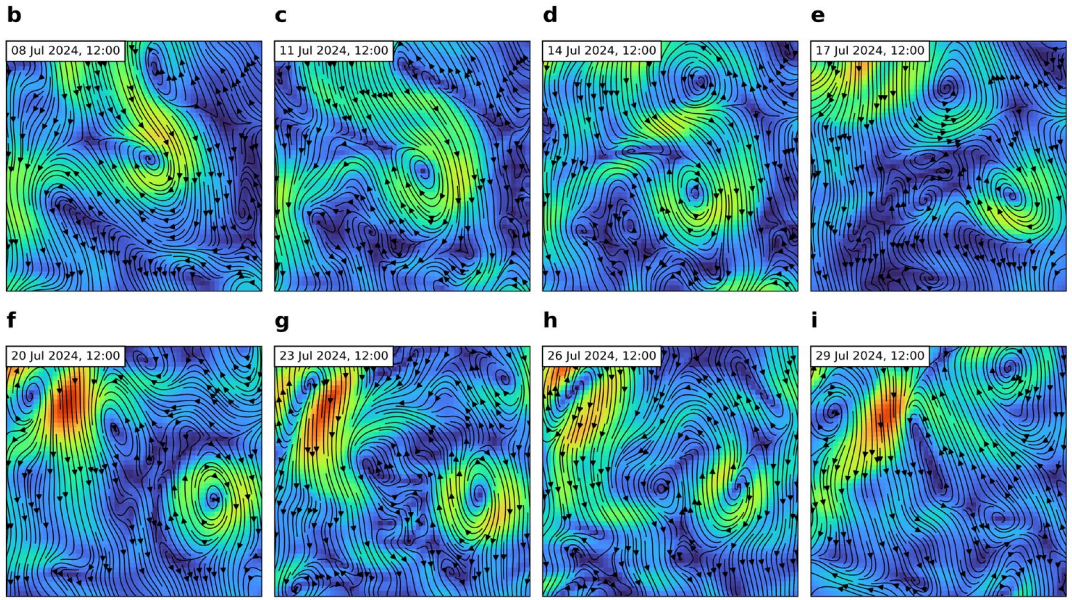

QG-model (with SWOT)

DUACS (nadir only)

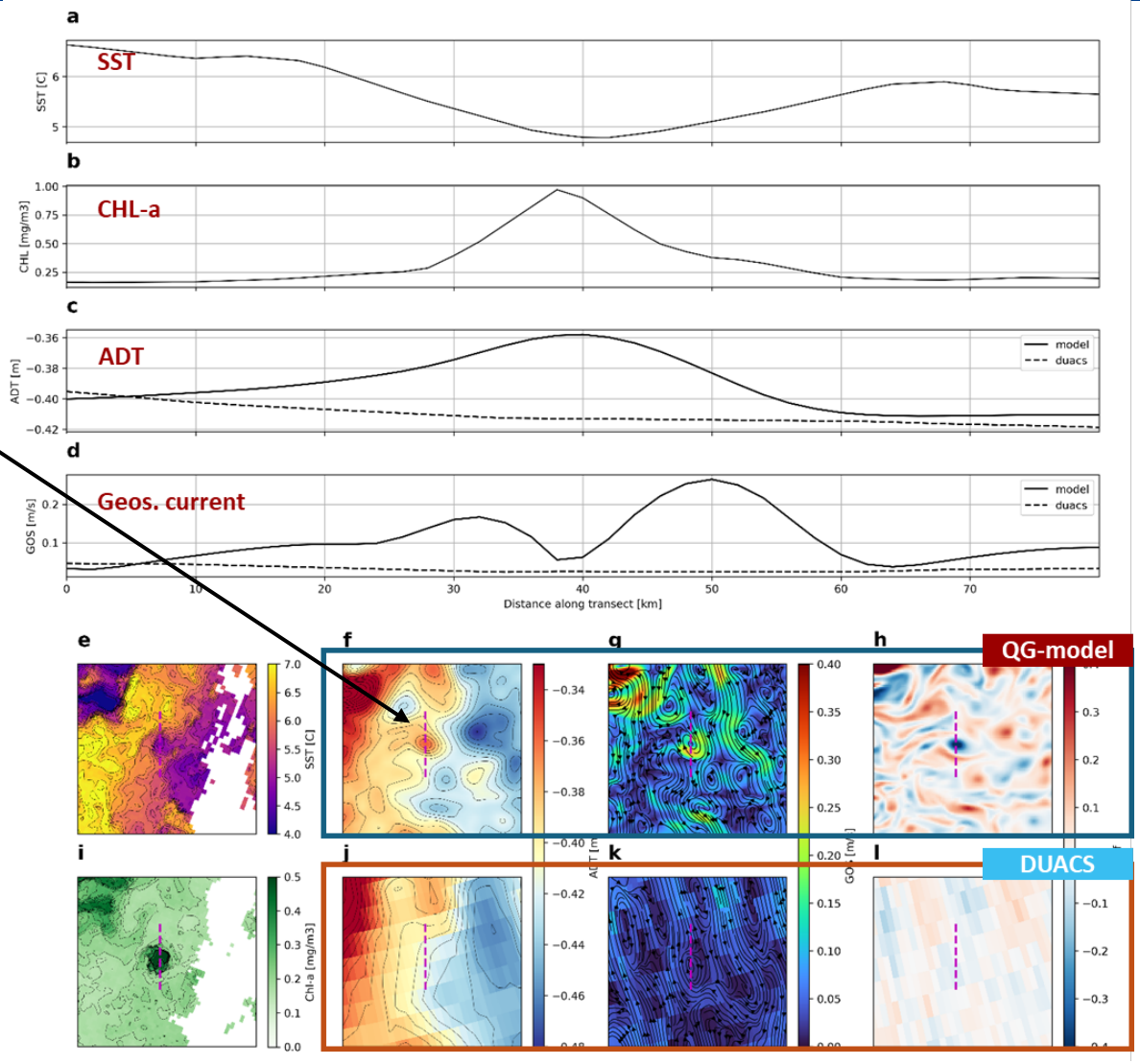
# Detecting a 30 km eddy




Small anticyclonic mesoscale eddy seen in SST data is detected by the QG-model



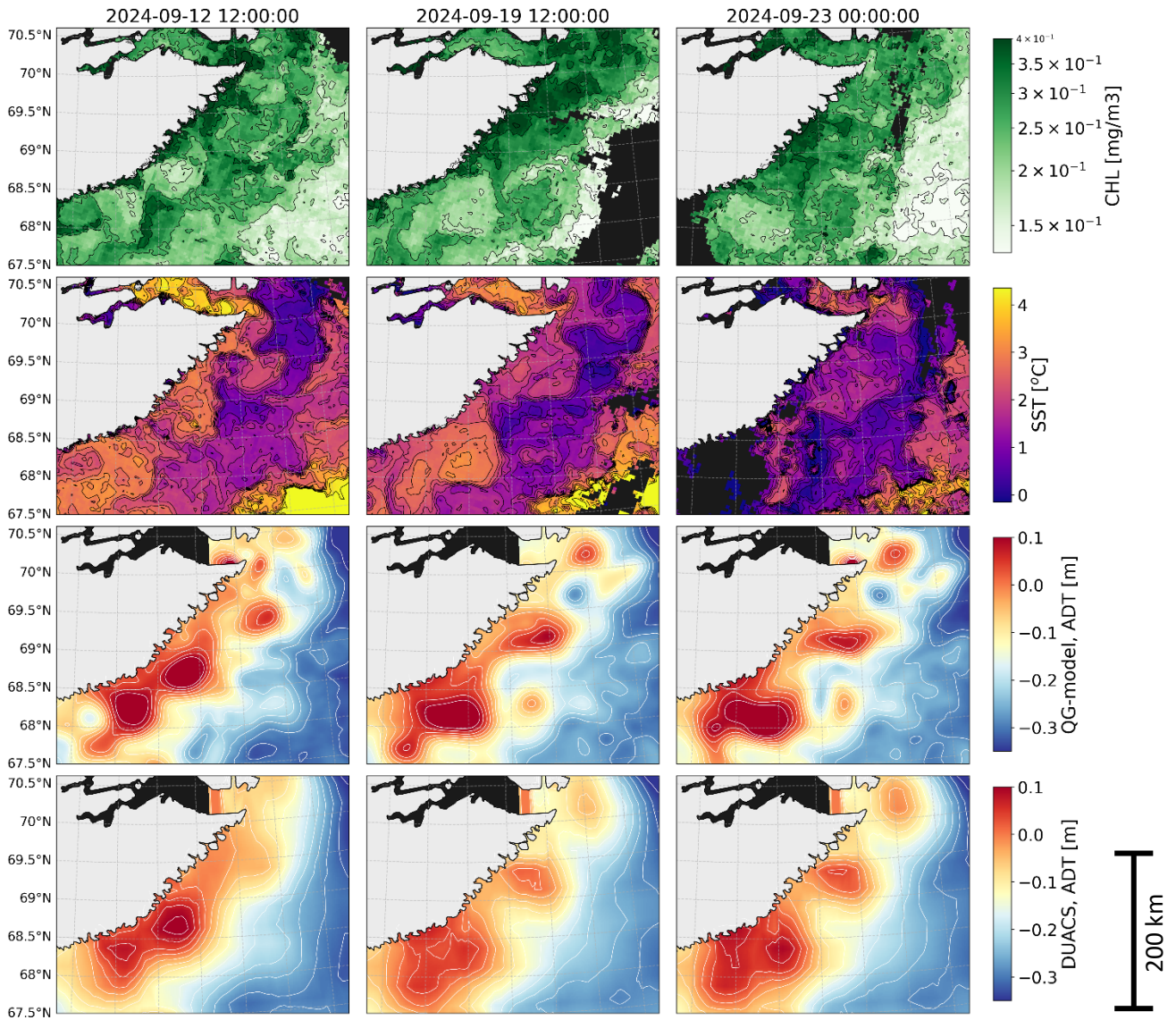

Eddy formation and breakup can be observed using the QG-model




- Diameter 30 km, amplitude 15 cm, Eddy is not detected by DUACS.
- Cold core and high chlorophyll-a levels.

# Comparison with SST and chlorophyll-a

- Front between EGC cold water and warm water from Scoresbysund.
- Excellent agreements in shapes for QG-model and SST.
- Smaller 30 km eddies are seen only in QG-model.
- Large 100 km eddies are resolved by DUACS and QG-model.



# European Young Scientists contributions in Dragon 6

| Name | Institution | Poster title | Contribution including period of research |
|---|---|---|---|
| Carsten Ludwigsen | Technical University of Denmark | | Sea level in the Arctic Ocean |
| Bjarke Nilsson | Technical University of Denmark | | Marine gravity recovery |
| Veng Tadea | Technical University of Denmark | | Mean sea surface |
| | | | |
| | | | |

European young scientists are involved in the study of altimetry data application on marine gravity, bathymetry, mean sea surface and submesoscale eddy.

# Chinese Young Scientists contributions in Dragon 6

| Name | Institution | Poster title | Contribution including period of research |
|---|---|---|---|
| Jie Sun | First Institute of Oceanography, Ministry of Natural Resources | Inversion Of The 3-D Subsurface Temperature Field In The Northwest Pacific Based On The Spatial-temporal Fusion Model | Reconstruction of subsurface 3D T/S, 2024-2028 |
| Qian Chen | First Institute of Oceanography, Ministry of Natural Resources | | Data fusion of multi-type altimeters , 2024-2025 |
| Rena Dong | First Institute of Oceanography, Ministry of Natural Resources | | Data fusion of multi-type altimeters , 2024-2026 |
| Haoran Gu | First Institute of Oceanography, Ministry of Natural Resources | | Reconstruction of subsurface 3D T/S, 2024-2028 |
| Yong Li | First Institute of Oceanography, Ministry of Natural Resources | | Reconstruction of 3D mesoscale eddy, 2024-2027 |
| Chenqing Fan | First Institute of Oceanography, Ministry of Natural Resources | | Processing of multi-type altimeters, 2024-2025 |
| Wei Cui | First Institute of Oceanography, Ministry of Natural Resources | | Extraction of submesoscale eddies, 2024-2028 |

Chinese young scientists are involved in the study of altimetry data processing and application on submesoscale eddy, reconstruction of subsurface 3D T/S and mesoscale eddy.

# Young Scientist Poster

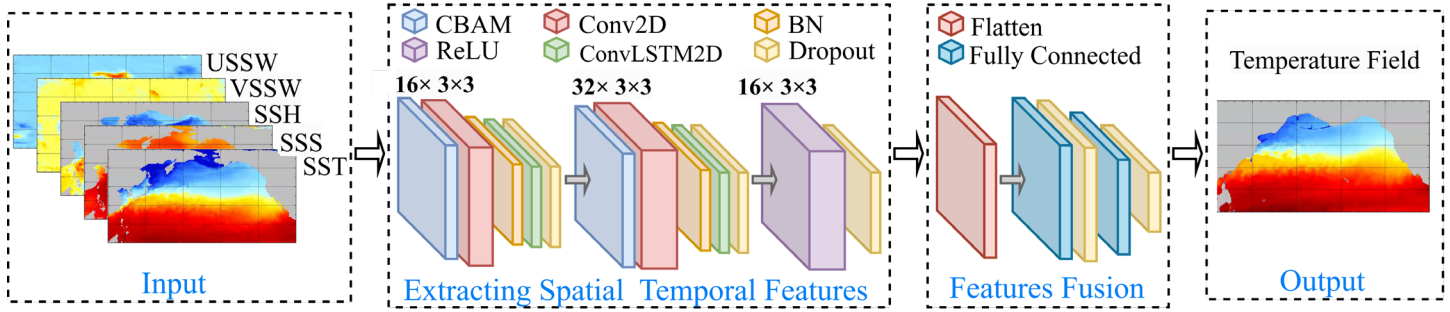
Poster Title: Inversion of The 3-D Subsurface Temperature Field in The Northwest Pacific Based on The Spatial-temporal Fusion Model

Authors: Jie Sun, Jungang Yang, Wei Cui

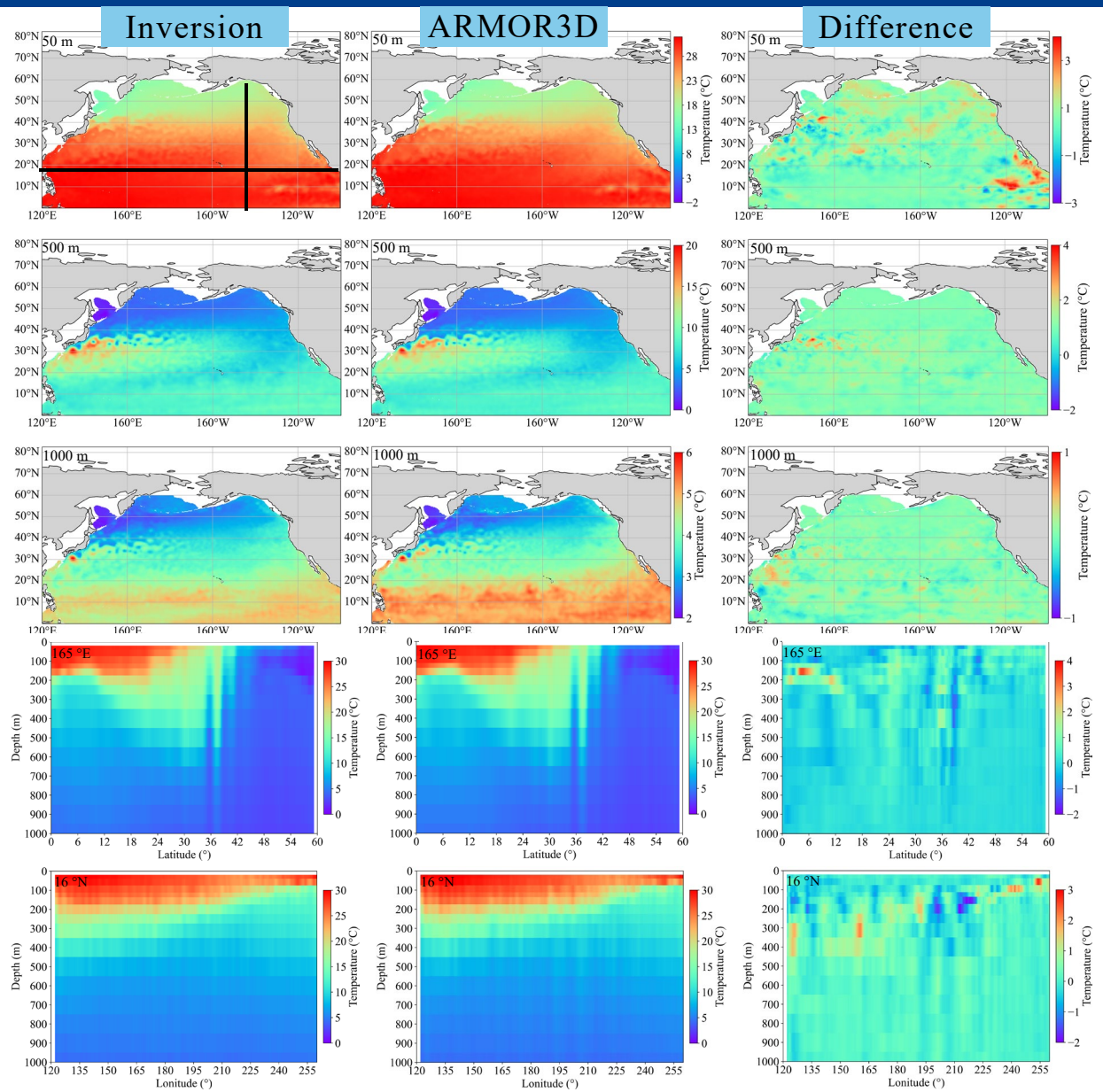
Abstract: this study develops a spatiotemporal fusion deep learning CNN-ConvLSTM model to reconstruct 3-D ocean subsurface temperature fields by multi-source satellite data. The proposed model is validated in the North Pacific by comparison with ARMOR3D temperature dataset. The results show that the proposed model effectively captures the spatial structures and temporal dynamics of the subsurface temperature field, achieving high consistency with observational data.

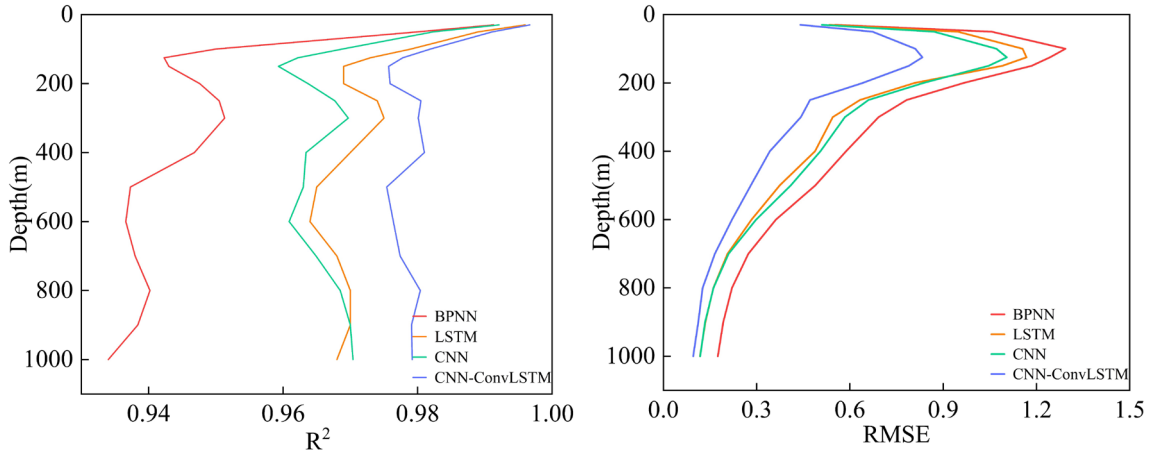
## CNN-ConvLSTM model

- Spatiotemporal feature extraction module.
- Feature fusion module.




| Data | Temporal resolution | Spatial resolution | Data source |
|---|---|---|---|
| SST | Daily | 0.05° | UKMO |
| SSS | Monthly | 0.125° | CMEMS |
| SSH | Daily | 0.25° | CMEMS |
| SSW | Monthly | 0.25° | CCMP |
| ARMOR3D | Monthly | 0.25° | CMEMS |



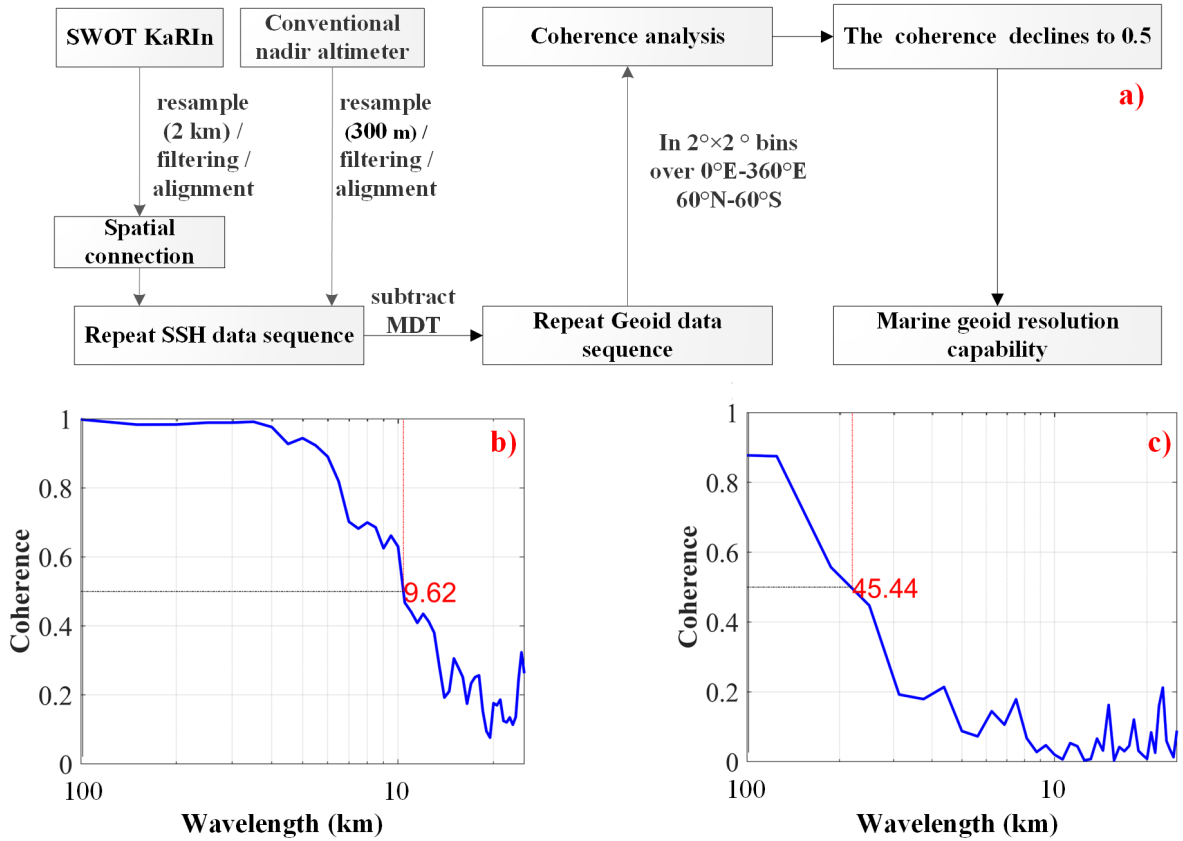




- The spatial distribution characteristics of the temperature can be well captured by CNN-ConvLSTM model, and The reconstructed temperature is relatively stable at different depths.
- CNN-ConvLSTM model shows better adaptability and robustness than other models.

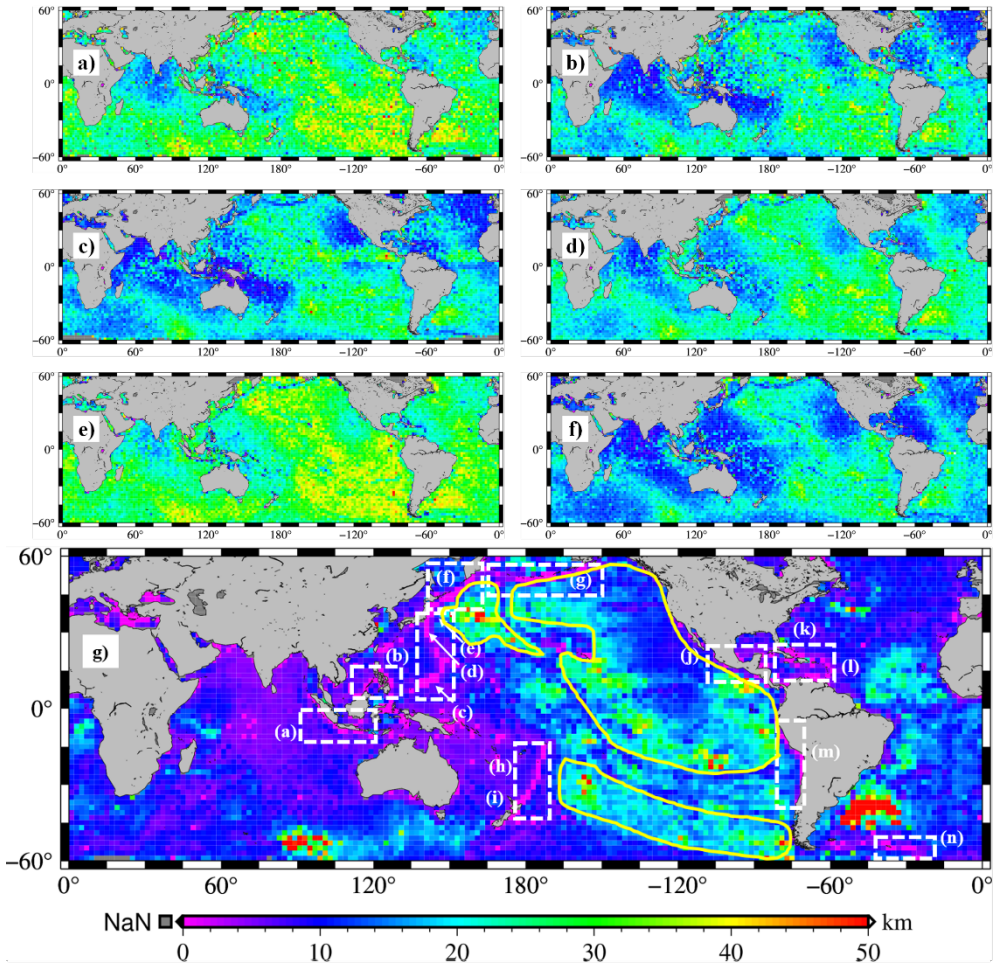
Poster Title: Along-track Marine Geoid Resolution Enhancement with SWOT

Authors: Shengjun Zhang, Xu Chen, Ole Baltazar Andersen, Yongjun Jia

Abstract: This study demonstrate the potential of SWOT Ka-band radar interferometer (KaRIn) to capture along-track short-wavelength signals below 10 km and analyze the bin-based statistics of key marine geophysical factors correlated with this marine geoid resolution capability.




Spectral analysis method (a) Flowchart; (b) Coherence declines to 0.5 at a wavelength of 9.62 km, where SWOT KaRIn exhibits better marine geoid resolution capability (2°E–4°E, 2°S–4°S); (c) Coherence declines to 0.5 at a wavelength of 45.44 km, where SWOT KaRIn exhibits poorer marine geoid resolution capability (266°E 268°E, 10°N–12°N).

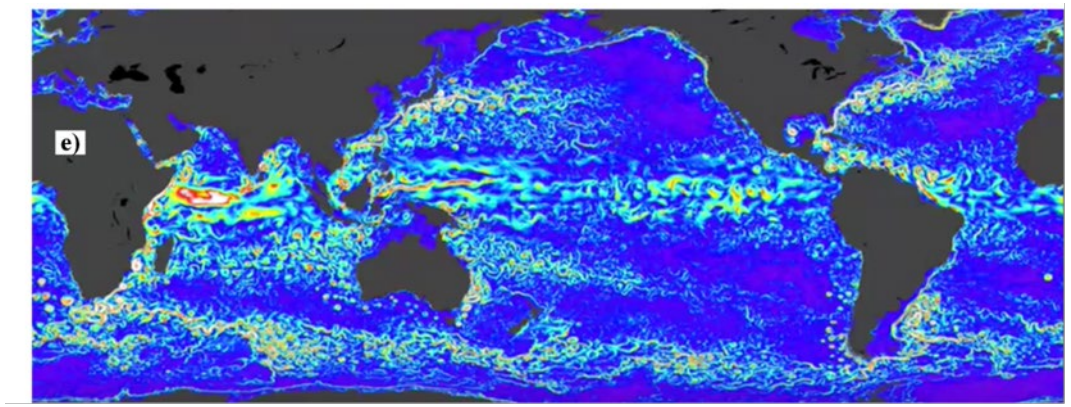



Marine geoid resolution capability of different satellites and bands (a: SWOT LRM C-Band; b: SWOT LRM Ku-Band; c: SARAL/AltiKa; d: Sentinel-3B PLMR Ku-Band; e: Sentinel-3B SAR C-Band; f: Sentinel-3B SAR Ku-Band; g: SWOT KaRIn).

**Table 1**

*Statistics Results of Marine Geoid Resolution Capability of Different Satellites and Bands*

| Satellite/Band | Grid number(pcs) | Non NaN grid number(pcs) | Max(km) | Min(km) | Mean(km) |
|---|---|---|---|---|---|
| SWOT KaRIn | 10,800 | 7,982 | 130.16 | 4.00 | 12.42 |
| SWOT Nadir C | 10,800 | 7,648 | 54.10 | 0.81 | 26.50 |
| SWOT Nadir Ku | 10,800 | 7,613 | 46.45 | 0.62 | 20.49 |
| Sentinel-3B SAR C | 10,800 | 7,921 | 49.95 | 0.63 | 28.21 |
| Sentinel-3B PLRM Ku | 10,800 | 7,827 | 43.47 | 1.01 | 22.03 |
| Sentinel-3B SAR Ku | 10,800 | 7,981 | 45.29 | 0.60 | 18.05 |
| SARAL/AltiKa Ka | 10,800 | 7,814 | 45.79 | 0.68 | 19.38 |




ocean current motion at 0.05° under SWOT observations, produced by JPL (JPL, 2014)

- SWOT has a significant improvement in marine geoid resolution capability, with an average enhancement of approximately 8 km.
- Short-wavelength geoid signals are more susceptible to ocean currents.

# Planning for the following year

- Data fusion of multi-type altimeters and altimetry data applications on ocean wave and marine gravity. (European side is for ocean wave, Chinese side is for marine gravity)
- Altimetry data application mean sea surface and Reconstruction of ocean subsurface 3-D temperature-salinity field. (European side is for mean sea surface , Chinese side is for 3-D temperature-salinity field)
- Altimetry data application submesoscale eddies/currents.  (Both sides)

# Training of young scientists

- The European and Chinese young scientists are trained for altimeter data processing and data applications on the marine dynamic environment monitoring.
- During September of 2024 DTU hosted the courses for the training of Young Scientists.
- The European young scientists will visit and work in the Chinese institute or university of Chinese partners for 1-3 months under the supporting from the ESA or the Chinese inviting funding.



CSTEC
中国科学技术交流中心
China Science and Technology Exchange Center

esa
THE EUROPEAN SPACE AGENCY

# Thank You